N.A.E.

R. & M. No. 2712
(12,114, 13,383)
A.R.C. Technical Report

MINISTRY OF SUPPLY

AERONAUTICAL RESEARCH COUNCIL
REPORTS AND MEMORANDA

The Design and Testing of Supersonic Nozzles

By

R. HARROP, P. I. F. BRIGHT,
J. SALMON and M. T. CAIGER

LONDON: HER MAJESTY'S STATIONERY OFFICE

1953

PRICE 10*s* 6*d* NET

The Design and Testing of Supersonic Nozzles

By

R. HARROP, P. I. F. BRIGHT, J. SALMON
and M. T. CAIGER

COMMUNICATED BY THE PRINCIPAL DIRECTOR OF SCIENTIFIC RESEARCH (AIR),
MINISTRY OF SUPPLY

Reports and Memoranda No. 2712†

May, 1950

Summary.—The theory of the flow through a throat near sonic velocity is developed, and is followed by a discussion of the conventional method of designing supersonic nozzles using the method of characteristics. A method of improving the Mach number distribution of the nozzle using the experimental results is developed.

The nozzles designed were tested in a 3-in. square wind tunnel in which the Mach number distribution was obtained by shaping the top wall of the working-section. The Mach number distribution along the bottom wall was determined from the pressures measured by a series of static pressure holes along the wall. Considerable difficulty was found in improving the distribution ; this was considered to be due to the discontinuity in curvature at the point of inflexion and the influence on the boundary layer of the sudden relaxation of the pressure gradient along the wall.

An alternative method of design was developed which avoided this discontinuity in curvature, and considerably better results were obtained when attempts were made to improve the experimental Mach number distribution.

The flow through the throat of the liners was determined experimentally and compared with the theory. The agreement was good on the whole, although there were differences in the subsonic entry region because the bottom wall only became flat a short distance before the throat.

In addition, tests were made which showed that the assumption of two-dimensional flow through the throat was justified.

The method developed to improve the distribution in the nozzle was extended to derive liner shapes for Mach numbers differing by 0·10 from the design Mach number. It was found that changes of this order could be made fairly successfully but further modification was necessary to reach the standard required for tunnel use.

The necessity for a smooth and accurately constructed liner surface is stressed. The limitations of the methods used for designing supersonic nozzles are discussed and several problems are mentioned which it is thought will need further consideration.

1. *Flow Through a Throat.*—1.1 *Introduction.*—Before the method of characteristics could be applied to the design of a nozzle, it was necessary to obtain a series of points near the throat at which the Mach number and the direction of flow were known.

It was decided that, instead of assuming that the sonic line and neighbouring lines of constant Mach number were straight, a linearised form of the equations of motion should be used to determine more accurately the nature of the flow in this region.

A discussion of the flow through a two-dimensional nozzle with sonic velocity at the throat has been given by Sauer[1]. The x axis was taken as the line of symmetry of the flow *i.e.*, the straight streamline, while the origin was the point at which sonic velocity a^* was reached on that line (Fig. 1).

† R.A.E. Reports Aero. 2293 and 2293a—received 29th January, 1949, and 14th September, 1950.

Let the velocity components of the flow be U, V, and assume that the flow is irrotational. Then, if

$$U = (1 + u)a^* \quad .. \quad .. \quad .. \quad .. \quad .. \quad .. \quad .. \quad (1)$$

$$V = va^* \quad .. \quad .. \quad .. \quad .. \quad .. \quad .. \quad .. \quad .. \quad (2)$$

there is a function ϕ such that $u = \partial\phi/\partial x$, $v = \partial\phi/\partial y$.

Near the origin the potential equation was shown, correct to first order to be expressible in the form :—

$$(\gamma + 1)\, u\frac{\partial u}{\partial x} - \frac{\partial v}{\partial y} = 0. \quad .. \quad .. \quad .. \quad .. \quad .. \quad (3)$$

By assuming that

$$\phi = [f_0(x) + y^2 f_2(x) + y^4 f_4(x) + \ldots, .] \quad .. \quad .. \quad .. \quad (4)$$

where $\left(\frac{\partial u}{\partial x}\right)_y = 0 = \eta$ *i.e.*, $(f'_0)_{y=0} = \eta x$, η being small, Sauer obtained the formulae :—

$$u = \eta x + \frac{(\gamma + 1)}{2}\eta^2 y^2 \quad .. \quad .. \quad .. \quad .. \quad .. \quad .. \quad (5)$$

and

$$v = (\gamma + 1)\,\eta^2 xy + \frac{(\gamma + 1)^2}{6}\eta^3 y^3 \quad .. \quad .. \quad .. \quad .. \quad .. \quad (6)$$

1.2. *Construction of Curves of Constant Mach Number.*—Equations 5 and 6 were used as a basis for the computation of constant Mach number curves. Along such a curve

$$(1 + u)^2 + v^2 = \text{constant} = (1 + u_0)^2 \quad .. \quad .. \quad .. \quad .. \quad .. \quad .. \quad (7)$$

where u_0 was the value of u at the point where the required Mach number M was reached on the x axis.

Since $$(1 + u_0) = \frac{U_0}{a^*} = \frac{U_0}{a_s}\frac{a_s}{a^*}$$

(where a_s is equal to the speed of sound in the gas after isentropic deceleration to rest) the value of u_0 for any M was found using the tables of Refs. 2 and 3.

Substitution into (7) from (5) and (6) gave

$$y^2 = \frac{A - 2\eta x - \eta^2 x^2 *}{(\gamma + 1)\eta^2}$$

where A was a constant depending on M.

Curves were constructed for Mach numbers at intervals of 0·05 in the range 0·80 to 1·30. The points for which the flow is parallel to the x-axis lie on a curve given by the equation $v = 0$, which is called the ' peak ' curve; this gives the position of the throat for each streamline.

* Just prior to publication, the authors were informed that the term $\eta^2 x^2$ in the above expression arose through an inconsistency in the order of the approximation used. This affects Fig. 1 and the related tables, but not the main results which are concerned with the alternative method of design and the improvement of the Mach number distribution by using the experimental results. The experimental determination of the Mach number distribution near the nozzle throat shows that the error involved in the approximation seems to have little adverse effect and may have given a better approximation than the true first-order theory.

1.3. *Construction of the Streamlines.*—The position of the streamlines was found by a step-by-step method, the spacing being chosen so that the fluid between consecutive ones would, if moving with sonic velocity, form a uniform stream of width 0·2 units.

For constant 'x' the ordinate of each streamline was found from that of the previous one, by using a mean Mach number (estimated from the previous curves) to determine the width B of the normal cross-section of the enclosed fluid[2,3].

A mean angle of flow ψ was computed from the inclination of the stream to the x-axis which was approximately $\tan^{-1} v/(1 + u)$.

Thus the intercept was of length $B/\cos \psi$.

The approximations used in finding the constant Mach number curves and streamlines were valid only in a small area surrounding the origin but the results are more accurate than one-dimensional theory in a larger area.

The co-ordinates for points on the streamlines for a range of values of x are given in Table 1 and their intersections with curves of constant Mach number, together with the direction of flow at those points in Table 2. The flow directions were first found for each streamline at fixed values of x by differencing the streamline ordinates, and then interpolated to give the values for the points of intersection with the Mach number curves.

2. *Design of Nozzles.*—2.1. *Determination of the Theoretical Nozzle Profile.*—A mathematical approach to the method of characteristics is given in Ref. 4 while a physical development is given in Ref. 5.

In the second of these references it is shown that the characteristics are inclined to the local direction of flow at any point in the stream, at the local Mach angle; also along characteristics arising from one wall A' is constant while B' is constant along those arising from the other wall. A' and B' are called the flow co-ordinates and are defined as $A' = \frac{1}{2}(P' + D')$ and $B' = \frac{1}{2}(P' - D')$ where P' (the pressure number) is equal to (1,000— Prandtl-Meyer angle in degrees)[6] and D' is the local stream direction (using an arbitrary datum).

It was also explained, how, given a series of initial points at which the values of P' and D' were known, further points could be determined and the Mach number and direction found throughout the field of flow. Fig. 2 illustrates this method by showing the construction of the point (A_1', B_2') from the points (A_1', B_1') and (A_2', B_2'). Each characteristic is inclined to the mean direction of flow across it at the Mach angle corresponding to the mean pressure number along it. (In the drawing $\mu_{P'}$ denotes the Mach angle corresponding to a pressure number P').

For the design of the first group of nozzles it was decided that the initial points should be taken on a curve of constant Mach number and that the throat should consist of a parabola with the same throat curvature as one of the streamlines (that corresponding to a sonic width of 3·6 units)*. The curve for Mach number 1·20 was chosen so that in the construction all characteristics should be on the downstream side of the initial points, and the direction of flow at its points of intersection with alternate streamlines was taken from Table 2 and, for convenience, corrected to the nearest 1/5 degree.

Fig. 3 is a reduction of the design drawing of a liner for Mach number 2·00 together with a table of values of A', B', P' and D' at the points of intersection of characteristics; some of the lines of the original drawing have, however, been omitted to avoid congestion. Only the portion of the flow above the axis of symmetry was considered. New points on this axis could be determined since, for such a point, the co-ordinates A' and B' were equal to one another and to the B' co-ordinate of the point from which the characteristic was to be drawn. Hence mean co-ordinates along the characteristic were known and its direction could be found and its position of intersection with the axis determined.

* For this streamline the value of the ratio $\frac{\text{radius of curvature of throat}}{\text{width of throat}} \simeq 4 \cdot 5$.

(52567) A 2

After the point 1 (Fig. 3) the curved wall of the nozzle could be arbitrarily chosen, the choice influencing the velocity distribution downstream of the characteristic through 1 and also the length of the nozzle from the throat to the point where the required Mach number is attained on the axis of symmetry.

It was decided that the parabola boundary, which had formed the throat, should be continued, thus ensuring a smooth wall, A characteristic was constructed to meet it, by first determining the approximate position of its intersection with the wall, and the values of A' and B′ for that point. (Since A' was constant along the characteristic its value was known; also, $(A' - B')$ was the direction of the wall which could be found from the equation of the parabola.) Thus the mean slope of the characteristic could be calculated and a more accurate position of intersection found. If necessary, an evaluation of the wall direction at this revised point enabled the process to be repeated and a better approximation to the position of the characteristic to be obtained.

The above method was continued until a point was reached on the curved wall for which the second co-ordinate was less than or equal to $\frac{1}{2}P'$ (where P' was the pressure number corresponding to the required Mach number). Linear interpolation enabled the point at which the value was exactly $\frac{1}{2}P'$ to be determined. After this point, the wall profile was found by using the condition that at any point its inclination should be such as to enable the second co-ordinate there to be $\frac{1}{2}P'$. This implied that, after the characteristic RR_1, one set of characteristics (those arising from the axis of symmetry) were straight. The flow was uniform downstream of the ' reflection ' in the axis of symmetry of the characteristic arising from the point of inflexion (or R_1R_2 in the figure). The inflexion occurs between 17 and 25.

The Cartesian co-ordinates of points on the nozzle wall were found by direct measurement of the axial ones and computation of the others from these and the mean wall direction between consecutive points (found from the D' co-ordinates). The theoretical nozzle exit width was found from the throat width[3] making allowance for the variation of Mach number across the throat by finding the ratio $\frac{\text{actual throat width}}{\text{sonic stream width}}$ from the results of section 1.3. This allowance was necessary since the tables are based on one-dimensional theory; that is, the Mach number across any cross-section is assumed uniform.

It was found that in each case the ratio $\frac{\text{working-section width} - \text{throat width}}{\text{throat width}} = t$, was within 1 per cent of the theoretical value T.

The value of $\frac{y - \text{throat width}}{\text{throat width}}$ at points of the wall was found and multiplied by T/t, giving revised co-ordinates with the correct area ratio.

The accuracy of this graphical method (t/T between 0·99 and 1·01) was considered sufficient to justify its use instead of the more laborious method of direct computation.

2.2. *Boundary-Layer Corrections.*—By integration of the momentum equation of the boundary layer Tetervin obtained[7], the equation

$$\left(\frac{\theta}{c}\right)_{s/c} = \frac{1}{(U/U_0)} H + 2\left[\frac{(1+n)k}{R_c^n}\int_{s_0/c}^{s/c}\left(\frac{U}{U_0}\right)^{(H+1)(n+1)+1} d(s/c) + \left(\frac{\theta_0}{c}\right)^{n+1}\left(\frac{U_1}{U_0}\right)^{(H+2)(n+1)}\right]^{\frac{1}{1+n}} \quad . . \quad (8)$$

where U was the local stream velocity outside the boundary layer, U_0 a standard velocity, U_1 the velocity at the point where integration commenced; s the distance along the surface, its initial value being s_0, c a standard length; θ the momentum thickness of the boundary layer with θ_0 the initial value, H the value of the ratio $\frac{\text{displacement thickness of boundary layer } (\delta)}{\text{momentum thickness of boundary layer } (\theta)}$, with H_0 the

initial value. τ_0 was the skin friction/unit area, q the dynamic pressure ($\frac{1}{2}\rho U^2$), ν the coefficient of kinematic viscosity, R_c the Reynolds number (based on c and U_0), and k and n constants in the assumed relationship $\tau_0/2q = k\nu^n/\theta^n U^n$. Their values depended on the type of boundary layer considered.

2.3. *Improvement of Mach Number Distribution from Experimental Results.*—Owing to the approximations made in the design of the nozzle and the estimation of the boundary-layer thickness it was thought that the Mach number distribution obtained from experimental tests of the nozzles would not be as good as might theoretically be expected. In consequence, a method was developed for the correcting of liner profiles from the experimental Mach number distribution along the axis of symmetry of the nozzle.

If a change $\delta\alpha$ is made in the inclination α at a point P of the liner, the Mach number at the intersection R of the characteristic from P with the axis of symmetry is increased by an amount $-2\frac{dM}{dP'}\delta\alpha$ while the increment in Mach angle μ is given by $-2\frac{d\mu}{dP'}\delta\alpha$ degrees where the derivatives are taken for the values of M and μ at R, and μ and α are measured in degrees.

This follows from Fig. 4, where the flow co-ordinates at P and R are $\{A', A' - \alpha\}$ and $\{A' - \alpha, A' - \alpha\}$ initially, and $\{A', A' - (\alpha + \delta\alpha)\}$ and $\{A' - (\alpha + \delta\alpha), A' - (\alpha + \delta\alpha)\}$ after the correction has been applied.

Using the relationship[5] $P' = 1000 - f(\mu)$ where $f(\mu) = \mu + \lambda^{-1}\tan^{-1}(\lambda\cot\mu) - 90°$ and $\lambda = \{(\gamma - 1)(\gamma + 1)\}^{1/2}$ by differentiation and substitution of $\gamma = 1{\cdot}400$, it is found that $\frac{d\mu}{dP'} = \frac{6 + \cot^2\mu}{5\cot^2\mu}$ and $\frac{dM_R}{d\alpha} = \frac{2}{57{\cdot}3}\left\{\frac{6+\cot^2\mu}{5}\right\}\sec\mu$.

Suppose an increment $[M]_x$ is required at R and that P is at a distance x from the beginning of the liner (Fig. 5), then the required change in inclination of the wall at P in radians is $\delta\alpha = K[M]_x$ where $K = 2{\cdot}5\{\cos\mu/(6 + \cot^2\mu)\}$, and thus if $[M]_x = 0$ for $x < x_0$, as a first approximation the increment in tunnel width for the point x is $\int_{x_0}^{x}\delta\alpha\sec^2\alpha\,dx = \int_{x_0}^{x}K[M]_x\sec^2\alpha\,dx$.

Generally $\sec^2\alpha$ may be taken equal to 1.

If the characteristic $A' =$ constant, at P comes from a point R' on the bottom wall, at which a correction to the Mach number has also to be applied, the correction for R' must be subtracted from the value of $[M]_x$ obtained from the curve.

3. *Experimental Work on the Original Nozzles.*—3.1. *Description of 3-in. Wind-Tunnel Working-Section.*—The theory developed in sections 1 and 2 was applied to design the liners for a 3-in. supersonic wind tunnel, of which the working section and contraction were similar to those proposed for a larger wind tunnel. The side walls of the wind tunnel from the end of the contraction to a point about 5 in. downstream of the working-section consisted of flat parallel sheets of $\frac{3}{8}$-in. glass while the bottom wall was flat and parallel to the wind tunnel centre-line from a distance of 3·6 in. after the exit of the contraction.

The static-pressure distribution along this wall could be found by means of pressure holes arranged at $\frac{1}{4}$-in. intervals on alternate sides of its centre-line and $\frac{1}{4}$ in. from it.

The contraction of the wind tunnel (Fig. 6) is described in Ref. 8. Its side walls became parallel before the exit, but the top and bottom walls finished at an angle of about 23 deg to the axis. The tunnel base was faired in to the contraction as a free streamline for incompressible flow derived from the equations of Ref. 9.

The co-ordinates are given in Table 3. Fig. 7 is a photograph of the working-section.

3.2. *Calculation of Liner Co-ordinates.*—For the application of the theory to the wind tunnel the flat wall was taken as the axis of symmetry. (A check on the validity of this assumption is given in sections 5 to 7 of the report.) The theoretical profile was scaled to a working-section width of 3 in. (or 6 in. for a symmetrical nozzle) and by means of graphical interpolation the values of y found for evenly spaced values of x.

In addition the parabola was faired in to the exit of the contraction. This enabled the position of the throat to be fixed. To give a good approximation to asymmetric flow it was kept as far downstream as possible allowing for the required position by which uniform flow should be attained.

It was decided that a boundary-layer allowance corresponding to the total laminar displacement thickness allowance required by all four walls should be applied to the top wall.

Using equation (8) assuming a uniform increase of velocity from the last screen in the contraction to a mean throat position and using a mean value of H obtained from Ref. 10, the boundary-layer thickness at the throat was found taking the initial thickness as zero. After the throat uniform rates of increase of velocity were used up to R and from R to R_2 (Fig. 3) for the top wall and from the throat to R_1 for the bottom wall. After R_2 and R_1 the velocity was assumed constant. The side wall allowance was taken as the mean of those found for the top and bottom walls.

The displacement thickness for the liner for Mach number 2·00 is shown in Fig. 8. For comparison, the unused results of calculations based on turbulent flow theory are also given. The total allowance in the latter case was found, however, to be nearer to that which it was later necessary to apply.

The laminar allowances were applied to the liner co-ordinates and a small alteration made to the fairing in to the contraction to allow for the change in throat co-ordinate.

3.3. *Use of One-Sided Liners.*—The decision to use one-sided liners instead of the conventional type was made because of several advantages which could be obtained. Instead of needing two curved walls for each Mach number only one would be required, also the common flat wall would be easier to make to the necessary accuracy, and could remain in position when the Mach number was varied, a great advantage on a larger wind tunnel. All corrections or alterations could be applied to the curved wall while the fixed wall could be used for pressure-plotting work particularly during liner design.

Use of the method causes a considerable increase in the minimum length of liner from throat to working-section and also a probable small change in stream inclination along the working-section.

3.4. *Initial Tests of Original Nozzles.*—The Mach number at points along the wall was computed from the static-pressure distribution assuming constant total head[2,3]. The air passing through the wind tunnel was dried by cooling to about — 25 deg C. and there was no evidence of condensation when the schlieren of the flow were observed with optical apparatus. At a sensitivity such that heat waves rising from a hand held near to the wind tunnel could be clearly seen, the effect of the sudden change in the velocity gradient at the point of inflexion was noticed, though no sharply defined shock-waves were visible at any Mach number.

The theoretical and experimental Mach number distributions are shown in Figs. 9 to 13. The additional curves in Figs. 10 to 12 were obtained from later re-design of the liners. The results for most pressure holes agreed to within 0·005 in Mach number with trial results obtained using an asymmetrical contraction in which the side and bottom walls were similar. Under those conditions it was more reasonable to assume that the bottom wall was the axis of symmetry of the flow through the throat.

It will be observed that agreement with theory was, in general, good for low supersonic Mach numbers but that the experimental results then fell below those expected. After a point corresponding approximately to the position of the characteristic from the point of inflexion, the

Mach number decreased over a distance of one or two inches and then commenced again to increase. In each case the mean Mach number was low, probably due to an underestimated boundary layer.

3.5. *Effect of Re-design.*—Three of the liners were re-designed to improve the Mach number distributions. When the total correction required by section 6 had been applied, it was generally necessary to scale the nozzle (equally in both directions) in order that the y co-ordinate at the diffuser end (where the wind-tunnel width was 3·000 in.) might be correct. For this purpose the x axis was taken as the flat wall and the y axis made to pass through the throat. Thus the y co-ordinate of the throat was generally altered but the x co-ordinate was unchanged. It was then necessary to fair the scaled parabola in to the contraction exit.

The experimental results from the re-designed liners are shown in Figs. 10, 11, 12 and 14. In the first three of these, in order that a direct comparison might be made with the theoretical curves and the initial distributions, a correction has been applied to the x co-ordinates to allow for the change in the scale of the nozzle.

It is seen that the distribution was unchanged over the first 8 in. of the bottom wall, at points where no correction had been applied. This illustrates that it is possible in practice to alter the nozzle profile at points on the top wall without affecting the flow upstream of the characteristic through the first of these points.

In Fig. 14 the curves are plotted without the application of a scale allowance to the x co-ordinates, *i.e.*, the distribution of Mach number is compared with that obtained from the same positions on the bottom wall in the initial tests.

Subsequent application seemed to indicate that the difficulty in obtaining a good Mach number distribution was caused by the conditions at the point of inflexion, since very small changes in inclination there were found to produce considerable changes both in the values and distribution of Mach number along the flat wall.

It is considered that this was probably due to the influence of the sudden expansion of the boundary layer caused by the relaxation of the pressure gradient at this point.

In the differential equation $\frac{d\theta}{ds} + \frac{H+2}{U}\frac{dU}{ds}\theta = \frac{kv^n}{U^n}\theta^{-n}$ from which equation (8) was derived, the expansion corresponds to the term $\frac{H+2}{U}\frac{dU}{ds}\theta$.

From the tests it appears that the increase in thickness was more than the theoretical, resulting in a local decrease in the effective inclination of the wall and a local isentropic compression or a very small oblique shock-wave. This was followed by an expansion as the rate of boundary layer increase fell more nearly to the theoretical value. Observation of the flow schlieren indicated a sudden increase in thickness near the point of inflexion.

Further re-design was done on the liners for Mach numbers 1·60 and 1·80 and the results after three re-designs are shown in Fig. 15. It was found that the improvement in Mach number had been accompanied by a gradual smoothing of the discontinuity in curvature. It was considered that the standard of uniformity of flow then reached in these two cases could not be raised much higher by using these methods of design and re-design.

The liner template co-ordinates for each Mach number are given in Table 4 and the conventions used in the measurement of x and y are illustrated in Fig. 16.

3.6. *Experimental Technique.*—During the tests it was found essential that the nozzles should have a smooth surface and should be constructed very accurately. For ease of construction and alteration the nozzle liners were made of wood; some of compressed wood and the others of teak.

It was found that if the surface was not completely Phenoglazed, shock-waves usually occurred from the uncovered portions of the wall. Wood which was polished but to which no Phenoglaze had been applied was completely unsuccessful, since shock-waves occurred and the pressure distribution was entirely different from that which was obtained with the liner Phenoglazed but unaltered in shape.

The accuracy to which the profiles were constructed was $\pm 0{\cdot}001$ in. The necessity for this was illustrated by the fact that the difference in throat co-ordinates between the first and third re-designs of the liner for Mach number 1·60 was 0·002 in., while the maximum change was 0·010 in. The difference in distribution can be seen by comparing Figs. 14 and 15.

3.7. *Discussion of the Results of Tests on the Original Liners.*—The application of re-design to improve the initial results was not completely successful, although a general agreement with theory was obtained. The chief cause of the difficulties found, seemed to be associated with conditions near the point of inflexion, where, if the method of design described above is used, there is a discontinuity in curvature: this leads to a rapid thickening of the boundary layer. It was thought possible that better results might be obtained if a method of design could be used which avoided this discontinuity.

The final results obtained from the liners are tabulated below:—

Theoretical Mach number	Mean Mach number	Variation about mean	State of liner
		(per cent.)	
1·40	1·353	±2·04	Initial state. Could be considerably improved by re-design.
1·60	1·606	±1·09	Third re-design. The liner is approaching the limit of accuracy obtainable by the method. There is evidence to indicate that most of the difficulties are due to conditions near the point of inflexion.
1·80	1·799	±1·41	As 1·60 liner.
2·00	2·04	—	First re-design. The liner could be improved by re-design, but was unsatisfactory since the Mach number reached its peak value almost 2 in. after the desired position. For this reason no variation figure is given.

It should be noticed that the Mach number variations and mean Mach numbers are given over a distance of not less than 7 in. on the bottom wall.

4. *Alternative Method for Design of Nozzles.*—4.1. *Determination of Theoretical Nozzle Profile.*—In an attempt to overcome the inflexion difficulties which occurred with the original liners, an alternative method was developed avoiding the curvature discontinuity and a new set of liners designed. The first of these was for a Mach number of 1·60, and since the same initial points were used as for the original liner, the velocity distribution up to the characteristic through P_0 (determined by the curved wall profile up to P_0 and the flat wall, Fig. 17) is the same as in the former case.

A velocity distribution was chosen along the bottom wall, downstream of the point 152, which satisfied the following conditions:—

(a) It should fair-in with the distribution from the origin to the point 152.

(b) It should reach the required Mach number (1·60) at a point far enough upstream for the velocity to be uniform at the working section.

(c) The approach to this Mach number should be smooth.

Using the method of characteristics, it was now possible to determine the flow downstream of 1, 152 from the conditions along that line and the portion 152, 194 of the flat wall; for example, the flow co-ordinates of the point 153 were known from those of 152 and 161, and hence by drawing lines through these points at directions corresponding to mean co-ordinates, the position of 153 was determined. From 143, 153 the point 144 was found, and so on.

The nozzle profile was found as the streamline of this flow which passed through P_0. The direction of flow at P_0 (Figs. 17 and 18) was 4 deg, at points 2 and 4 it was 4·9 deg; hence the mean direction of the portion P_0 of the wall was 4·45 deg, and K could be determined. Since the direction of the wall in the next portion (to the characteristic 4, 5) was known to be slightly over 5 deg, a line was drawn at 5 deg through K and the inclination of the stream to the datum at its point of intersection L′ with 4, 5 was calculated by linear interpolation of the directions of flow at these two points. Hence a more accurate estimation of the mean direction and the position of the wall (L) could be made.

The wall was drawn up to the characteristic 38, 194 and afterwards, was determined by a simple wave. A uniform stream was obtained downstream of 194, 195. To increase accuracy, the Cartesian co-ordinates of each point on the wall, were found in the same way as in the case of the original liners.

There are several ' a priori ' difficulties in this method; for example, the characteristics might meet before the curved wall is reached, or the resultant wall shape be re-entrant.

If care is taken in the choice of the initial points these difficulties can be avoided. If desired, a rough check of the positions of characteristics and wall inclinations can be made by using a few of the initial points as starting points for a subsidiary drawing before commencing the main design.

The alternative method requires a longer length of liner to reach a desired Mach number, using the same throat curvature, than the original method. For this reason smaller throat radii of curvature were used for liners for Mach numbers 1·80 and 2·00, to increase the rate of increase of velocity along the bottom wall in the neighbourhood of the throat. The initial points are shown in Fig. 19 the co-ordinates being given in Table 5. For the liner for Mach number 1·40 the points were again chosen on axial and perpendicular lines but with a different throat curvature. Although, in general, the point of inflexion occurred at the beginning of the simple wave this was not a necessity, as illustrated in the case of the liner for Mach number 1·40, where the wall, though concave to the stream, was an expansion surface. The possibility of this occurring was shown in Ref. 5 and is illustrated in Fig. 20 where a Prandtl-Meyer expansion round a corner is shown. If a wall is placed between the streamline and the straight wall, it is possible that an expansion will occur. Near P there is definitely an expansion, but further away it would require a full drawing to find the conditions at any particular point.

The liner for Mach number 1·60 was scaled and a boundary-layer allowance was applied as for the original liners; the others had a linear allowance the amount being chosen from comparison with those experimentally required for the original liners.

Due to the increased throat curvatures used in the design of the liners for Mach numbers 1·80 and 2·00 it was found difficult to fair-in the parabola to the contraction without having the throat further upstream than would have been satisfactory considering the assumption that the bottom wall was the axis of symmetry of the flow.

A slightly different parabola which faired-in more easily to the contraction, was used upstream of the throat for the construction of these liners and although this would have affected the initial points, they would still be more accurate than points given by one-dimensional flow, while any small variations caused in Mach number could theoretically be improved by re-design.

4.2. *Initial Tests on the Alternative Liners.*—The results of the initial tests on the liners are shown in Fig. 21. It will be noticed that there were no appreciable pressure decreases in the neighbourhood of the characteristics through the point of inflexion but that the amplitude of Mach number variation was very little different from that previously obtained.

The fact that the mean Mach number was approximately correct for each liner except Mach number 1·60, and in that case was similar to the value obtained in the initial test of the corresponding original liner, suggested that the total boundary-layer allowance which it was necessary to apply was almost unchanged. No sharply defined shock-waves either in the working-section or arising from the point of inflexion were visible by the schlieren method even at full sensitivity.

4.3. *Re-design Tests of the Alternative Liners.*—Before mathematical re-design was applied to the alternative liner for Mach number 1·60 it was decided to apply a linear correction to raise the Mach number to approximately 1·60. Together with the liners for Mach numbers 1·80 and 2·00 it was then re-designed following the theory of 2.3. A further re-design was required for the liner for Mach number 1·60.

The considerably improved distributions are shown in Fig. 22 and it is particularly noticeable that the conditions near the inflexion characteristic are more satisfactory since there were no serious unexpected changes in the distribution of Mach number. This was probably due to the gradual relaxing of the pressure gradient on the boundary layer and the consequent less abrupt thickening of the layer compared with the previous case.

Agreement between the initial, re-design and theoretical Mach number distributions up to the point at which alterations were applied was, as with the original liners, very good.

A test was made on a liner with shape approximating to the original liner for Mach number 2·00 but with a smooth change in curvature near the inflexion. This gave a smooth but far from uniform Mach number distribution, the variation being of the order of 5 per cent.

Table 6 gives the template co-ordinates of the liners after re-design, the axes being illustrated in Fig. 16.

The final variations are given in the table below.

Theoretical Mach Number	Mean Mach Number	Variation about Mean	State of Liner
		(per cent.)	
1·40	1·402	±0·50	Initial.
1·60	1·600	±0·52	Third re-design. (One of the re-designs was linear).
1·80	1·801	±0·42	First re-design.
2·00	2·002	±0·60	First re-design.

5. *Experimental Determination of the Flow through a Sonic Throat.*—5.1. *Introduction.*—The linearised theory of the flow through a sonic throat was fully developed in section 1, and the curves of constant Mach number (M) and the streamlines there obtained are shown in Fig. 1. The assumptions made were strictly valid only near the point where sonic speed was reached along the straight streamline but it was thought that an approximation to the flow conditions better than that given by one-dimensional theory would be obtained over a considerably greater area.

The Mach number distribution in the sonic region of the 3-in. wind-tunnel was measured by pressure plotting on the side and bottom walls, to check the following two assumptions made in the theory:—

(a) That the flow in the throat is two-dimensional. This assumption is reasonable, since the side walls of the wind tunnel become parallel about five inches before the throat.

(b) That the bottom wall of the wind tunnel is a plane of symmetry. This assumption, which is essential for the theory, cannot be exact because the bottom wall, which is faired-in from the contraction, only becomes flat a short distance before the throat. This lack of symmetry might be important, particularly at lower Mach numbers, and experimental verification was needed.

5.2. *Description of the Pressure-Plotting Walls.*—For the tests one of the glass side-walls of the wind tunnel was replaced by a wall made of compressed wood which had 180 static-pressure holes spaced evenly over an area 4·8 in. × 3 in. in the neighbourhood of the throat (Figs. 23 and 24). The surface of the wood in contact with the flow was lacquered with Pheenorock and carefully smoothed so that shock-waves should not arise from it and, to prevent surface irregularities, the static holes were drilled with a No. 76 drill, leakage through the laminations of the wood being avoided by coating the inside of the holes with Pheenorock. Copper tubes, sealed into the wood, connected the holes to a distributor board.

In order to check whether the assumption of two-dimensional flow was valid, a wooden bottom wall was prepared with 50 pressure-plotting holes evenly spaced near the position of the throat (Figs. 23 and 24).

5.3. *Description of Tests on the Side and Bottom Walls.*—Tests were made on the original liners for Mach numbers 1·40, 1·60 and 2·00 and the 'alternative' liner for Mach number 1·60. Since there were insufficient manometer tubes to enable all the static pressures to be read simultaneously, a number of runs were made on each liner, the pressures at four fixed holes being read in each case to check the consistency of the results. The Mach number distribution was computed assuming constant total head. It was always found that the Mach numbers at the four fixed holes agreed to within 0·3 per cent.

The curves of constant Mach number (Fig. 25), have been obtained by linear interpolation between measurements at adjacent holes. The pronounced scatter of the points forming the curves of constant Mach number for values of 0·90, 0·95 and 1·20 in the case of the liner for Mach number 1·40 and also the liners for Mach number 1·60 (Fig. 25), is due to a few holes being consistently in error. The interpolation procedure used to obtain lines of constant Mach number involves using each reading several times, and one faulty pressure hole thus affects a large number of points. If these readings are omitted, the interpolated points lie close to the mean curve as drawn. The pressure holes were re-drilled before tests were made on the liner for Mach number 2·00 and the irregularities do not occur.

The results of the pressure-plotting of the bottom wall for the liner for Mach number 2·00 (Fig. 26), show that the assumption of two-dimensional flow is justified.

The theoretical distributions for the liners (Figs. 27, 28, 29 and 30) have been obtained from Fig. 1 for the constant Mach number lines up to 1·20 and then from the design drawings of the liners by interpolation of pressure numbers.

5.4. *Discussion of the Side-Wall Results.*—The theoretical and experimental results for the above liners are compared in Figs. 27, 28, 29, and 30, the drawings being scaled to constant throat width. The point where the bottom wall becomes flat is marked in each case. Since the liners had the same value for the ratio $\frac{\text{throat radius of curvature}}{\text{width of throat}}$, the theoretical Mach number distributions up to the curve for Mach number 1·20 were the same.

The effect of the initial curvature of the bottom wall (where the bottom wall is faired-in to the contraction) is very noticeable for, at the lower Mach numbers, the curves for constant Mach number tend to be symmetrical about the centre-line of the contraction. After the curve for Mach number 0·90, however, the theoretical and experimental results agree better. In the cases of the original liners for Mach numbers 1·40 and 1·60, the last of the theoretical curves changes direction abruptly near the curved wall of the nozzle, at the point where the characteristic from the point of inflexion intersects the curve of constant Mach number. The experimental results show the same tendency, but the position of the mean curve is not very well defined owing to inaccuracies of interpolation in a region of almost constant Mach number.

Because a suitable velocity distribution, which avoided a sudden change of curvature at the point of inflexion, was used for the alternative liner for Mach number 1·60, there is no corresponding abrupt change of direction in the theoretical curve for Mach number 1·35 in this case. Figs. 8 and 9 show clearly the differences in distribution between the original and alternative liners for Mach number 1·60, the rapid acceleration of the air stream after reaching a Mach number of 1·20 and the sudden change in direction of the theoretical curve for Mach number 1·35 in the case of the original liner (Fig. 29) contrasting strongly with the more gradual acceleration obtained from the alternative liner (Fig. 30).

Considering the range of Mach number over which the linear theory was applied, the agreement between the theoretical and experimental results was good.

6. *Modifications to Liners to Change the Mach Number.*—Following the success of the application of the method of modifying a liner shape to correct the measured pressure distribution, an attempt was made to alter the Mach number of the 1·60 alternative liner to 1·50 in this way. Since only a first-order approximation is given to the required increment in tunnel width, the method strictly should not be applied to produce such a large change in Mach number, but, in view of its simplicity compared with the design of a new liner, it was thought worth while to see if changes of this order could be made satisfactorily.

The Mach number distribution, which is shown in Fig. 31 is in fact better than those obtained from the initial tests on the existing alternative liners (Fig. 21). The following additional liner shapes were then derived, in each case from the design for a higher Mach number so that the position of the working section would be satisfactory:—

$M = 1{\cdot}90$ from the $M = 2{\cdot}00$ alternative liner,

$M = 1{\cdot}70$ from the $M = 1{\cdot}80$ alternative liner,

and $M = 1{\cdot}30$ from the $M = 1{\cdot}40$ alternative liner.

In all cases the new liners were derived from the design drawings of the old liners before modifications were made to improve the velocity distributions. The Mach number distributions for these are also shown in Fig. 31. The mean Mach numbers and the percentage variations from the mean are tabulated below:—

Design M	Mean M	Maximum per cent Variation
1·30	1·295	±1·31
1·50	1·500	±1·00
1·70	1·700	±1·29
1·90	1·91	±0·76

These results show that it is possible to alter the design Mach number of a liner by amounts up to 0·10 and still maintain a reasonable distribution. Further modification, based on the measured pressure distribution, is necessary, however, to reach the standard achieved in the case of the basic liners.

A new difficulty occurs in calculating these modifications as there are no design drawings available for use in determining the relationship between the top and bottom walls*, but an approximation to this relationship can be obtained by comparing those for higher and lower Mach numbers. The comparison should be made between corresponding portions, such as the part of the wall from the point of inflexion to the point where uniform flow begins. (The inclination of the characteristic from the point of inflexion can be found by interpolation, while its

i.e. the points on the top wall which are on the same characteristics as given points on the bottom wall, *see* Ref. 1.

reflexion makes the Mach angle of the flow with the bottom wall. Uniform flow begins where this characteristic meets the top wall.) The relationship found in this way is more accurate than that used to derive the liner shape from the design of a previous liner, although a mean wall correspondence computed as above could have been used as a refinement of the method.

The best results obtained from the liners up to date are shown in Fig. 32 and are summarised below :—

Design M	Mean M	Maximum per cent. Variation	State of liner
1·30	1·310	±0·58	2nd modification
1·50	1·498	±0·93	1st modification
1·70	1·698	±1·09	5th modification
1·90	1·906	±0·69	2nd modification

It is seen that very little improvement has been made to the distributions. This is shown for example in the results for the liner for Mach number 1·70. The difficulties found in this case are probably due to the presence of several shock waves in the initial tests. The alterations involved in the modifications were generally less than 0·010 in. in wind-tunnel width at all points of the nozzles.

6.1. *Discussion of Results.*—The application of the method of calculating the necessary modifications to liner shapes is limited by the accuracy to which it is practicable to specify the ordinates. In the present method of liner construction, metal templates are made to the given co-ordinates to tolerances of ± 0·001 in. The liner is then worked to shape until the surface is within 0·001 in. of the template at all points. In the finishing process the liner is rubbed in a longitudinal direction to make its surface as smooth as possible. The tolerances on the ordinates may produce variations in the slope of the liner, and the effect of these on the Mach number distribution can be calculated from the equations of section 2.3. It is found that the possible irregularities of Mach number are of the same order as those measured in the wind tunnel, which shows that further improvement in the Mach number distribution cannot be expected until the technique of liner construction has been improved.

The method of determining the Mach number distribution used in these tests, *i.e.*, pressure-plotting the flat wall, was chosen because it was very convenient for the method of calculating the necessary modifications to the liner shape, since disturbances are known to arrive from points on the shaped wall. It was assumed that if a good distribution was obtained over a sufficient length of the flat bottom wall (about three tunnel widths), then the distribution in the stream was probably satisfactory.

Before the liners are considered suitable for wind-tunnel use, a full exploration of the working-section distribution should be made. It should be borne in mind, however, that if modifications are needed to improve a static-traverse measured in the stream, it may not be easy to determine the origin of a weak disturbance which may not show on schlieren photographs.

7. *Conclusions.*—It is considered that the time taken in the accurate determination of the theoretical nozzle profiles was justified since, although the boundary-layer allowances were not estimated correctly, the initial Mach number distributions were quite good and considerably better than could be expected from less accurate methods.

The cause of the difficulties found in improving the distribution seemed to be associated with conditions near the point of inflexion and the effect on the boundary layer of a sudden change in pressure gradient. It was found that with a smooth change of curvature at the point of inflexion, the results of the attempts to improve the Mach number distribution were more nearly in accordance with theory.

The final results on the alternative liners show that, over a distance of about $2\frac{1}{3}$-tunnel heights along the bottom of the tunnel, it is possible to obtain variations of about $\pm \frac{1}{2}$ per cent. from the theoretical design Mach number. The average rate of increase of boundary-layer displacement-thickness along the tunnel, based on the difference between the theoretical and experimental throat widths, was of the order of 0·002 to 0·003 in./in./wall.

Although the linear theory of the flow through a sonic throat is valid only close to the point where the flow becomes sonic on the bottom wall, and, on the nozzles tested, the throat is near the point where the bottom wall becomes flat, good agreement has been obtained between the theoretical and experimental results, while the experimental results also show that the flow through the throat is very closely two dimensional.

Provided that a change of not more than 0·10 in Mach number is required, a good first approximation to the liner shape can be obtained from one of higher Mach number. Further modification is necessary however, to achieve a standard comparable to the basic liners. This proved to be difficult and comparatively little improvement was made.

A very smooth nozzle surface is required, and since wood was used, Phenoglazing was necessary. A very high standard of accuracy had to be maintained during construction ($\pm$ 0·001 in.) since very small variations in co-ordinates affected the Mach number distribution even in the case of the alternative liners. It is thought that further work will require greatly improved constructional and experimental techniques.

There remains a wide field of investigation which has not received much attention such as the theoretical and experimental investigation of the influence of the sonic line on design, and the evaluation of boundary-layer thickness.

REFERENCES

No.	*Author*	*Title, etc.*
1.	R. Sauer	General Characteristics of the Flow Through Nozzles in Neighbourhood of the Critical Velocity. A.R.C. 9499. September, 1944. (Unpublished.)
2.	D. E. Lindop and E. E. Regan	Tables for Compressible Air Flow Calculations. Part 2. A.R.C. 9933. March, 1946. (Unpublished.)
3.	D. E. Lindop, E. E. Regan and R. Harrop.	Tables for Compressible Air Flow Calculations. Part 3. A.R.C. 11,118. March, 1947. (Unpublished.)
4.	G. Temple	The Method of Characteristics in Supersonic Flow. R. & M. 2091. January, 1944.
5.	R. Harrop	An Introduction to the Method of Characteristics. R.A.E. Aero. Rep. 2275. A.R.C. 11,974. July, 1948. (To be published in *Aircraft Engineering*, August, 1953.)
6.	R. Harrop	Tables for Compressible Air Flow Calculations. Part 5. R.A.E. Tech. Note Aero. 1738d. A.R.C. 11,236. November, 1947. (Unpublished.)
7.	N. Tetervin	A Method for the Rapid Estimation of Turbulent Boundary Layer Thicknesses for Calculating Profile Drag. A.R.C. 8498. March, 1945. (Unpublished.)
8.	R. Harrop	Method for Designing Wind Tunnel Contractions. A.R.C. 11,603. March, 1948. *J.R.Ae.S.* March, 1951.
9.	G. Greenhill	Theory of a Streamline past a Plane Barrier and of the Discontinuity Arising at the Edge with an Application to the Theory of an Aeroplane R. & M. 19. 1910.
10.	W. F. Cope	The Laminar Boundary Layer in Compressible Flow. A.R.C. 7635. November, 1943. (Unpublished.)

NOTATION

Flow through a Throat

x, y	Cartesian co-ordinates. x measured along the straight streamline from an origin at the point where sonic speed is reached
a^*	The speed of sound (and of the stream) at the point (0,0)
U, V	Components of velocity of the gas
u	$(U/a^*)-1$
v	V/a^*
ϕ	$u = \frac{\partial \phi}{\partial x}$, $v = \frac{\partial \phi}{\partial y}$, $\phi = f_0(x) + y^2 f_2(x) + y^4 f_4(x) + \ldots$
γ	Ratio of the specific heats of the gas (air; 1·400)
η	$(\partial u/\partial x)_{y=0}$
U_0, u_0	The values of U, u at a particular point on the x axis.
a_s	The speed of sound in the gas after isentropic deceleration to rest
A	A constant in the equation for the lines of constant Mach number
M	Mach number
B	The width of the normal cross-section of the fluid between two required streamlines
ψ	The mean angle of the flow, across a line of constant x, between two streamlines

Method of Characteristics

μ	Mach angle
P'	Pressure number. (1000-Prandtl-Meyer angle in degrees)
D'	Stream inclination to the axis of symmetry
A'	Flow co-ordinate $\frac{P' + D'}{2}$
B'	Flow co-ordinate $\frac{P' - D'}{2}$
$\mu_{P'}$	Mach angle corresponding to a pressure number of P'

Suffices $_{1, 2, 3}$ are used to indicate the values of these quantities at particular points.

Boundary Layer

U	Local stream velocity outside boundary layer (initial value U_1)
U_0	Standard velocity
s	Distance measured along the surface.
c	Standard length
θ	Momentum thickness of the boundary layer
δ	Displacement thickness of the boundary layer
H	δ/θ

τ_0	Skin friction/unit area
q	Dynamic pressure ($\frac{1}{2}\rho U^2$). (ρ density of the gas)
ν	Coefficient of kinematic viscosity
R_c	Reynolds number based on c, U_0
k, n	Constants in the assumed relationship $\frac{\tau_0}{2q} = \frac{k\nu^n}{\theta^n U^n}$

A suffix $_0$ is used to indicate the initial values of s, θ, δ and H.

Re-design

α	Inclination of the curved wall.
$[M]_x$	Required increment in M at the point x. (Fig. 5).
K	$2{\cdot}5\left(\frac{\cos\mu}{6+\cot^2\mu}\right)$.

TABLE 1

Flow through a Throat. *Co-ordinates of Streamlines*

The table gives the values of y corresponding to fixed values of x for evenly spaced streamlines

Sonic Width	$x = -2{\cdot}0$	$x = -1{\cdot}6$	$x = -1{\cdot}2$	$x = -0{\cdot}8$	$x = -0{\cdot}4$	$x = 0{\cdot}0$	$x = 0{\cdot}4$	$x = 0{\cdot}8$	$x = 1{\cdot}2$	$x = 1{\cdot}6$	$x = 2{\cdot}0$
0·2	0·2067	0·2043	0·2024	0·2011	0·2003	0·2000	0·2003	0·2011	0·2024	0·2042	0·2066
0·4	0·4134	0·4085	0·4047	0·4021	0·4005	0·4000	0·4006	0·4021	0·4047	0·4084	0·4133
0·6	0·6199	0·6126	0·6070	0·6031	0·6007	0·6000	0·6009	0·6032	0·6072	0·6128	0·6200
0·8	0·8263	0·8166	0·8092	0·8040	0·8009	0·8000	0·8012	0·8044	0·8097	0·8172	0·8270
1·0	1·0325	1·0204	1·0113	1·0048	1·0011	1·0000	1·0016	1·0057	1·0124	1·0219	1·0342
1·2	1·2384	1·2241	1·2132	1·2056	1·2012	1·2000	1·2020	1·2071	1·2152	1·2268	1·2417
1·4	1·4440	1·4275	1·4149	1·4063	1·4013	1·4001	1·4025	1·4086	1·4183	1·4319	1·4495
1·6	1·6493	1·6306	1·6165	1·6068	1·6014	1·6002	1·6032	1·6103	1·6216	1·6374	1·6578
1·8	1·8542	1·8335	1·8179	1·8072	1·8014	1·8003	1·8039	1·8122	1·8252	1·8433	1·8665
2·0	2·0587	2·0360	2·0191	2·0076	2·0014	2·0005	2·0048	2·0143	2·0291	2·0496	2·0758
2·2	2·2628	2·2383	2·2201	2·2078	2·2014	2·2008	2·2059	2·2168	2·2335	2·2565	2·2858
2·4	2·4665	2·4403	2·4209	2·4080	2·4015	2·4012	2·4073	2·4196	2·4384	2·4640	
2·6	2·6697	2·6420	2·6215	2·6081	2·6015	2·6018	2·6089	2·6228	2·6438	2·6722	
2·8	2·8726	2·8434	2·8220	2·8081	2·8017	2·8026	2·8109	2·8265	2·8498	2·8811	
3·0	3·0751	3·0445	3·0223	3·0082	3·0020	3·0037	3·0133	3·0308	3·0565	3·0910	
3·2	3·2773	3·2455	3·2226	3·2083	3·2025	3·2051	3·2161	3·2357	3·2641	3·3018	
3·4	3·4791	3·4462	3·4228	3·4085	3·4032	3·4069	3·4195	3·4413	3·4725	3·5138	
3·6	3·6806	3·6468	3·6230	3·6089	3·6043	3·6092	3·6235	3·6477	3·6820	3·7270	
3·8	3·8819	3·8473	3·8233	3·8094	3·8056	3·8120	3·8282	3·8550	3·8926	3·9416	
4·0	4·0830	4·0478	4·0237	4·0103	4·0075	4·0154	4·0338	4·0633	4·1045	4·1578	

TABLE 2

Flow through a Throat. Curves of Constant Mach Number

Mach number 0·90

x	y	Direction
−1·038	0·000	0·00
−1·042	0·202	−0·20
−1·057	0·404	−0·40
−1·078	0·606	−0·61
−1·109	0·808	−0·83
−1·148	1·010	−1·07
−1·198	1·213	−1·32
−1·254	1·417	−1·59
−1·322	1·621	−1·90
−1·402	1·826	−2·23
−1·493	2·032	−2·61
−1·594	2·238	−3·04
−1·704	2·447	−3·51
−1·827	2·658	−4·06
−1·968	2·870	−4·69
−2·119	3·084	−5·40
−2·287	3·302*	−6·19
−2·471	3·524*	−7·12
−2·676	3·748*	−8·16
−2·900	3·975*	−9·40
−3·151	4·210*	−10·84

Mach number 1·00

x	y	Direction
0·000	0·000	0·00
−0·004	0·200	0·00
−0·019	0·400	0·00
−0·037	0·600	−0·01
−0·063	0·800	−0·03
−0·100	1·000	−0·06
−0·142	1·200	−0·10
−0·194	1·401	−0·17
−0·254	1·601	−0·25
−0·325	1·801	−0·37
−0·404	2·001	−0·51
−0·490	2·203	−0·69
−0·587	2·405	−0·93
−0·691	2·606	−1·16
−0·806	2·808	−1·47
−0·931	3·013	−1·83
−1·066	3·218	−2·25
−1·214	3·424	−2·75
−1·381	3·634	−3·34
−1·561	3·845	−4·04
−1·754	4·061	−4·84

Mach number 1·10

x	y	Direction
0·987	0·000	0·00
0·984	0·201	0·18
0·973	0·403	0·36
0·954	0·605	0·54
0·927	0·806	0·70
0·896	1·007	0·88
0·856	1·208	1·01
0·806	1·408	1·13
0·750	1·609	1·25
0·684	1·810	1·32
0·613	2·010	1·38
0·533	2·209	1·42
0·448	2·409	1·43
0·351	2·608	1·38
0·244	2·807	1·30
0·132	3·007	1·18
0·009	3·205	1·00
−0·120	3·405	0·78
−0·260	3·605	0·50
−0·408	3·805	0·15
−0·572	4·007	−0·29

Mach number 1·20

x	y	Direction
1·923	0·000	0·00
1·920	0·206	0·37
1·908	0·412	0·73
1·889	0·618	1·09
1·863	0·824	1·45
1·832	1·029	1·79
1·793	1·234	2·12
1·746	1·438	2·44
1·693	1·642	2·74
1·628	1·845	3·01
1·560	2·048	3·26
1·485	2·250	3·48
1·402	2·451	3·68
1·313	2·652	3·83
1·213	2·851	3·94
1·106	3·050	4·02
0·992	3·249	4·05
0·871	3·447	4·04
0·742	3·644	3·99
0·605	3·841	3·86
0·460	4·038	3·67

Peak curve

x	y
−0·001	0·200
−0·005	0·400
−0·012	0·600
−0·021	0·800
−0·033	1·000
−0·047	1·200
−0·065	1·400
−0·084	1·600
−0·107	1·800
−0·132	2·000
−0·159	2·200
−0·190	2·401
−0·223	2·601
−0·258	2·801
−0·297	3·001
−0·337	3·202
−0·381	3·403
−0·428	3·604
−0·477	3·805
−0·529	4·007

* These points are on interpolated positions of streamlines the main calculations only being made up to $x = -2{\cdot}0$. They satisfy the equation for the curve of $M = 0{\cdot}90$.

TABLE 3

Co-ordinates of Tunnel Base

x Measured from beginning of liner section.

y Distance below tunnel centre-line.

x	y	x	y
0·00	2·150	2·20	1·538
0·20	2·044	2·40	1·528
0·40	1·936	2·60	1·519
0·60	1·828	2·80	1·513
0·80	1·743	3·00	1·508
1·00	1·688	3·20	1·504
1·20	1·646	3·40	1·502
1·40	1·613	3·60	1·500
1·60	1·588		
1·80	1·568		
2·00	1·551		

A locating flange of width $\frac{1}{2}$ in. was fitted between the end of the contraction and the beginning of the liner section.

(Note. Table 4 is on the next page.)

TABLE 5

Cartesian and Flow Co-ordinates for the Alternative Initial Points for the Method of Characteristics given in Fig. 19

Equation of parabola:

$$y = 10 + (0{\cdot}02463)\,(x + 1{\cdot}790)^2$$

Point	x	y	P'	D'	A'	B'
1	−1·620	10·004	996·50	0·50	498·50	498·00
2	−1·620	9·057	997·60	−0·40	498·60	499·00
3	−1·620	8·009	998·65	−1·35	498·65	500·00
4	−0·605	8·009	997·60	1·40	499·50	498·10
5	0·368	8·009	996·45	3·55	500·00	496·45
6	0·368	6·792	997·60	2·40	500·00	497·60
7	0·368	5·316	998·65	1·35	500·00	498·65
8	1·294	5·316	997·60	2·40	500·00	497·60
9	2·189	5·316	996·45	3·55	500·00	496·45
10	2·189	3·676	997·40	2·20	499·80	497·60
11	2·189	1·838	998·05	0·95	499·50	498·55
12	2·189	0·000	998·30	0·00	499·15	499·15

These values were obtained from the calculations of section 1 of the report.

TABLE 4

Template Co-ordinates of Original Liners

Liner A		Liner B		Liner C		Liner D	
x in.	y in.	x in.	y in.	x in.	y in.	x in.	y in.
0·000	0·475	0·000	0·475	0·000	0·475	0·000	0·475
0·090	0·523	0·240	0·604	0·100	0·529	0·060	0·504
0·390	0·685	0·540	0·765	0·400	0·690	0·360	0·661
0·690	0·846	0·840	0·927	0·700	0·851	0·660	0·792
0·990	1·007	1·140	1·088	1·000	0·997	0·960	0·894
1·290	1·169	1·440	1·249	1·300	1·114	1·260	0·982
1·590	1·330	1·740	1·388	1·600	1·220	1·560	1·062
1·890	1·491	2·040	1·508	1·900	1·318	1·860	1·135
2·190	1·653	2·340	1·610	2·200	1·408	2·160	1·200
2·490	1·814	2·640	1·703	2·500	1·488	2·460	1·257
2·790	1·975	2·940	1·787	2·800	1·560	2·760	1·308
3·220	2·190	3·240	1·861	3·100	1·623	3·060	1·350
3·520	2·268	3·540	1·925	3·400	1·677	3·360	1·386
3·820	2·320	3·840	1·980	3·700	1·722	3·660	1·413
4·120	2·361	4·140	2·026	4·000	1·759	3·960	1·434
4·420	2·390	4·440	2·063	4·300	1·787	4·260	1·447
4·720	2·407	4·740	2·090	4·600	1·806		
		5·040	2·107	4·900	1·816	4·600	1·452
5·020	2·413	5·340	2·115				
				5·100	1·818	4·860	1·450
5·185	2·411	5·450	2·116			5·160	1·441
5·477	2·399			5·197	1·817	5·460	1·424
5·769	2·377	5·635	2·114	5·488	1·811	5·760	1·399
6·061	2·343	5·926	2·103	5·778	1·795	6·060	1·374
6·352	2·298	6·217	2·082	6·069	1·772	6·360	1·349
6·644	2·243	6·509	2·053	6·359	1·740	6·660	1·325
6·936	2·176	6·800	2·014	6·650	1·702	6·960	1·301
7·227	2·108	7·092	1·966	6·941	1·664	7·260	1·279
7·519	2·042	7·383	1·911	7·231	1·623	7·560	1·258
7·811	1·977	7·675	1·857	7·522	1·582	7·860	1·238
8·103	1·915	7·966	1·805	7·812	1·542	8·160	1·220
8·394	1·854	8·257	1·754	8·103	1·504	8·460	1·204
8·686	1·796	8·549	1·704	8·394	1·470	8·760	1·189
8·978	1·740	8·840	1·657	8·684	1·438	9·060	1·177
9·270	1·685	9·132	1·613	8·975	1·405	9·360	1·166
9·561	1·635	9·423	1·569	9·265	1·375	9·660	1·157
9·853	1·586	9·715	1·525	9·556	1·346	9·960	1·150
10·145	1·541	10·006	1·484	9·847	1·320	10·260	1·145
10·437	1·498	10·297	1·445	10·137	1·295	10·560	1·141
10·728	1·457	10·589	1·409	10·428	1·273	10·860	1·138
11·020	1·418	10·880	1·377	10·718	1·253	11·460	1·137
11·312	1·382	11·172	1·346	11·009	1·234	12·060	1·135
11·603	1·348	11·463	1·317	11·300	1·217	12·660	1·133
11·895	1·316	11·754	1·290	11·590	1·202	13·260	1·132
12·187	1·287	12·046	1·267	11·881	1·189	13·860	1·130
12·479	1·261	12·337	1·247	12·171	1·179	14·460	1·129
12·770	1·236	12·629	1·229	12·462	1·170	15·060	1·128
13·062	1·215	12·920	1·213	12·753	1·163	15·660	1·126
13·354	1·195	13·212	1·197	13·043	1·157	16·250	1·125
13·646	1·177	13·503	1·184	13·334	1·152		
13·937	1·162	13·794	1·172	13·624	1·147		
14·229	1·149	14·086	1·163	14·206	1·139		
14·521	1·139	14·377	1·154	14·787	1·135		
14·813	1·133	14·669	1·147	15·368	1·130		
15·104	1·129	14·960	1·141	15·901	1·126		
15·396	1·127	15·252	1·135	16·250	1·125		
15·688	1·125	15·543	1·130				
15·979	1·125	15·941	1·127				
16·250	1·125	16·250	1·125				

Liner A :—First re-design $M = 2·00$.
Liner B :—Third re-design $M = 1·80$.
Liner C :—Third re-design $M = 1·60$
Liner D :—Initial design $M = 1·40$.

TABLE 6

Template Co-ordinates of Alternative Liners

Liner E		Liner F		Liner G		Liner H	
x in.	y in.	x in.	y in.	x in.	y in.	x in.	y in.
0·00	0·475	0·000	0·475	0·000	0·475	0·000	0·475
0·10	0·529	0·100	0·529	0·350	0·663	0·200	0·583
0·40	0·690	0·400	0·690	0·650	0·825	0·500	0·744
0·70	0·843	0·700	0·851	0·950	0·986	0·800	0·905
1·00	0·980	1·000	1·007	1·250	1·147	1·100	1·067
1·30	1·085	1·300	1·134	1·550	1·303	1·400	1·228
1·60	1·171	1·600	1·242	1·850	1·448	1·700	1·389
1·90	1·244	1·900	1·341	2·150	1·566	2·000	1·551
2·20	1·310	2·200	1·431	2·450	1·667	2·300	1·712
2·50	1·368	2·500	1·512	2·750	1·758	2·600	1·873
2·80	1·419	2·800	1·585	3·050	1·839	2·900	2·035
3·10	1·461	3·100	1·649	3·350	1·911	3·200	2·173
3·40	1·496	3·400	1·703	3·650	1·973	3·500	2·273
3·70	1·523	3·700	1·749	3·950	2·025	3·800	2·339
4·00	1·543	4·000	1·786	4·250	2·068	4·100	2·381
4·30	1·554	4·300	1·814	4·550	2·102	4·400	2·411
		4·600	1·834	4·850	2·126	4·700	2·429
		4·900	1·844	5·150	2·140		
4·60	1·558						
		5·100	1·846	5·450	2·145	5·000	2·435
4·90	1·552						
5·20	1·539	5·379	1·841	5·650	2·135	5·201	2·423
5·50	1·522	5·673	1·826	5·851	2·113	5·402	2·392
5·80	1·502	5·967	1·804	6·051	2·081	5·603	2·348
6·10	1·479	6·261	1·775	6·251	2·044	5·803	2·300
6·40	1·456	6·555	1·741	6·452	2·005	6·004	2·250
6·70	1·432	6·848	1·704	6·652	1·966	6·306	2·175
7·00	1·409	7·142	1·665	6·852	1·928	6·607	2·100
7·30	1·386	7·436	1·626	7·053	1·889	6·908	2·027
7·60	1·364	7·730	1·587	7·353	1·831	7·209	1·956
7·90	1·343	8·024	1·550	7·654	1·775	7·511	1·888
8·20	1·323	8·318	1·514	7·954	1·720	7·812	1·822
8·50	1·305	8·611	1·480	8·255	1·667	8·113	1·759
8·80	1·288	8·905	1·448	8·555	1·617	8·414	1·699
9·10	1·273	9·199	1·418	8·856	1·568	8·716	1·642
9·40	1·259	9·493	1·390	9·156	1·523	9·017	1·589
9·70	1·247	9·787	1·363	9·457	1·480	9·318	1·539
10·00	1·236	10·081	1·338	9·757	1·440	9·619	1·493
10·30	1·227	10·375	1·317	10·058	1·404	9·921	1·450
10·60	1·218	10·668	1·296	10·358	1·371	10·222	1·411
10·90	1·211	10·962	1·279	10·659	1·341	10·523	1·376
11·20	1·205	11·256	1·262	10·959	1·314	10·825	1·345
11·50	1·200	11·550	1·246	11·260	1·290	11·126	1·317
11·80	1·196	11·844	1·234	11·560	1·269	11·427	1·291
12·10	1·192	12·138	1·223	11·861	1·250	11·728	1·268
12·40	1·189	12·432	1·214	12·161	1·233	12·030	1·247
12·70	1·186	12·725	1·207	12·462	1·219	12·331	1·228
13·00	1·183	13·019	1·201	12·762	1·207	12·632	1·213
13·30	1·180	13·313	1·196	13·062	1·197	12·933	1·200
13·60	1·178	13·607	1·191	13·363	1·190	13·235	1·190
		13·901	1·188	13·663	1·184	13·536	1·181
		14·195	1·184	13·964	1·179	13·837	1·174
Straight		14·489	1·180	14·264	1·175	14·138	1·169
		14·782	1·177	14·565	1·172	14·440	1·166
20·00	1·125	15·076	1·174	14·865	1·169	14·741	1·163
		15·370	1·171			15·042	1·161
		Straight		Straight		Straight	
		20·000	1·125	20·000	1·125	20·000	1·125

Liner E :—Initial design $M = 1·40$.
Liner F :—Third re-design $M = 1·60$.
Liner G :—First re-design $M = 1·80$.
Liner H :—First re-design $M = 2·00$.

TABLE 7

Template Co-ordinates for $M = 1{\cdot}30$, $1{\cdot}50$, $1{\cdot}70$ and $1{\cdot}90$ Liners

$M = 1{\cdot}30$		$M = 1{\cdot}50$		$M = 1{\cdot}70$		$M = 1{\cdot}90$	
x in.	y in.	x in.	y in.	x in.	y in.	x in.	y in.
0·000	0·475	0·000	0·475	0·000	0·475	0·000	0·475
0·100	0·529	0·200	0·583	0·350	0·663	0·200	0·583
0·400	0·690	0·500	0·744	0·650	0·825	0·500	0·744
0·700	0·817	0·800	0·878	0·950	0·978	0·800	0·905
1·000	0·914	1·100	0·991	1·250	1·117	1·100	1·067
1·300	0·999	1·400	1·095	1·550	1·240	1·400	1·228
1·600	1·077	1·700	1·190	1·850	1·351	1·700	1·389
1·900	1·148	2·000	1·278	2·150	1·453	2·000	1·551
2·200	1·211	2·300	1·357	2·450	1·546	2·300	1·712
2·500	1·267	2·600	1·428	2·750	1·630	2·600	1·870
2·800	1·315	2·900	1·490	3·050	1·705	2·900	1·999
3·100	1·356	3·200	1·544	3·350	1·771	3·200	2·094
3·400	1·390	3·500	1·590	3·650	1·828	3·500	2·161
3·700	1·416	3·800	1·627	3·950	1·877	3·800	2·211
4·000	1·434	4·100	1·658	4·250	1·917	4·100	2·250
4·300	1·445	4·400	1·677	4·550	1·948	4·400	2·278
		4·700	1·690	4·850	1·970	4·700	2·295
				5·150	1·984		
4·600	1·449	5·000	1·694			5·000	2·300
				5·450	1·988		
4·912	1·443	5·295	1·688			5·215	2·287
5·225	1·430	5·605	1·673	5·664	1·977	5·430	2·254
5·537	1·414	5·916	1·650	5·878	1·954	5·646	2·210
5·849	1·395	6·227	1·621	6·093	1·923	5·861	2·163
6·161	1·375	6·537	1·588	6·307	1·887	6·077	2·115
6·474	1·356	6·847	1·554	6·521	1·851	6·399	2·043
6·786	1·337	7·158	1·520	6·735	1·815	6·722	1·971
7·099	1·318	7·468	1·486	6·949	1·778	7·045	1·901
7·411	1·302	7·779	1·453	7·163	1·741	7·368	1·833
7·724	1·286	8·090	1·421	7·484	1·687	7·690	1·768
8·036	1·272	8·399	1·391	7·805	1·635	8·013	1·706
8·348	1·259	8·710	1·364	8·127	1·585	8·336	1·646
8·661	1·248	9·021	1·339	8·448	1·537	8·659	1·590
8·973	1·238	9·331	1·314	8·769	1·491	8·982	1·537
9·285	1·230	9·642	1·293	9·090	1·448	9·305	1·488
9·597	1·222	9·952	1·274	9·411	1·409	9·628	1·443
9·910	1·216	10·262	1·257	9·732	1·374	9·951	1·402
10·222	1·211	10·573	1·242	10·054	1·342	10·273	1·365
10·534	1·206	10·884	1·229	10·375	1·312	10·596	1·332
10·846	1·203	11·194	1·219	10·696	1·285	10·919	1·303
11·159	1·200	11·504	1·210	11·017	1·262	11·242	1·277
11·471	1·197	11·815	1·202	11·339	1·243	11·565	1·255
11·783	1·193	12·125	1·197	11·661	1·226	11·888	1·236
12·097	1·190	12·436	1·194	11·982	1·212	12·211	1·220
12·409	1·187	12·747	1·191	12·303	1·201	12·534	1·206
12·721	1·183	13·056	1·188	12·624	1·192	12·856	1·195
13·033	1·180	13·367	1·185	12·945	1·186	13·179	1·186
13·346	1·178	13·678	1·181	13·266	1·182	13·502	1·179
13·658	1·175	13·988	1·177	13·588	1·178	13·825	1·174
13·970	1·173	14·299	1·173	13·909	1·175	14·147	1·169
14·282	1·170	14·609	1·170	14·230	1·171	14·470	1·165
14·595	1·168	14·919	1·167	14·551	1·167	14·793	1·162
14·907	1·166	15·230	1·165	14·872	1·164	15·116	1·159
15·219	1·163	15·541	1·163	15·193	1·161	15·439	1·156
15·532	1·161	15·852	1·161	15·514	1·159	15·762	1·154
15·844	1·158	16·162	1·159	Straight		Straight	
16·156	1·156	16·473	1·157	20·000	1·125	20·000	1·125
Straight		16·784	1·155				
20·000	1·125	17·094	1·152				
		Straight					
		20·000	1·125				

These liners are : Second modification $M = 1{\cdot}30$.
First modification $M = 1{\cdot}50$.
Fifth modification $M = 1{\cdot}70$.
Second modification $M = 1{\cdot}90$.

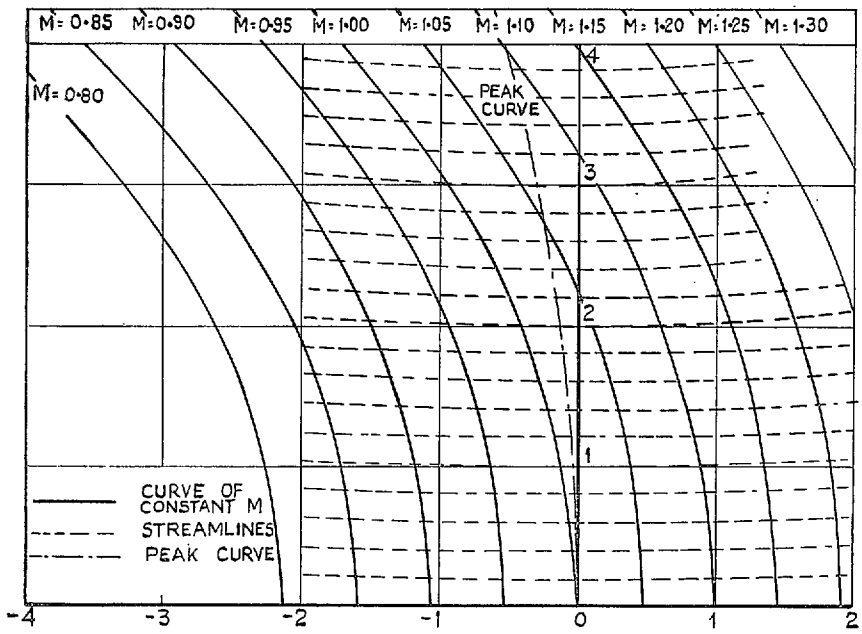

FIG. 1. Flow through a sonic throat.

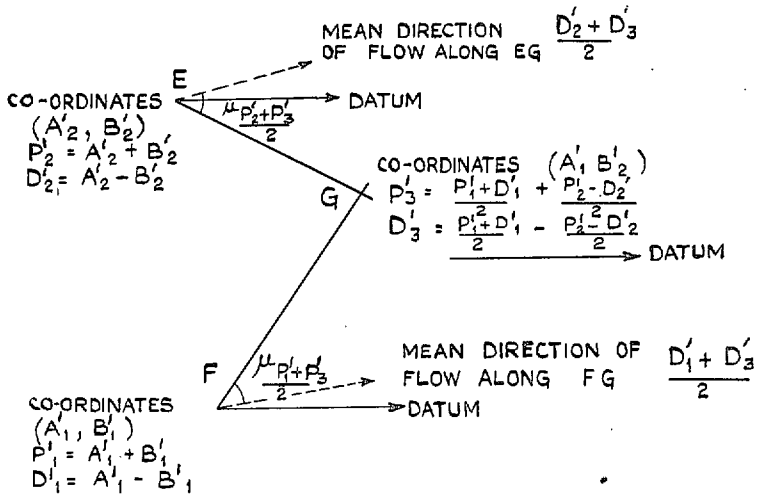

FIG. 2. Construction of characteristics.

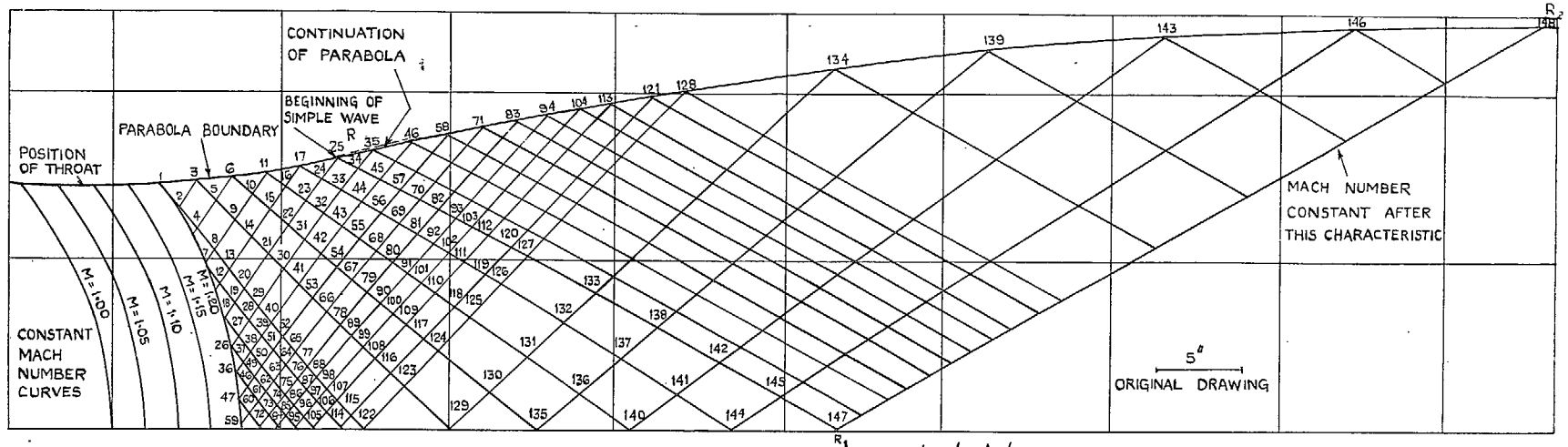

TABLE OF VALUES OF A′, B′, P′, D′.

PT	A′	B′	P′	D′
1	500·2	496·2	996·4	4·0
2	500·2	496·2	996·4	4·0
3	500·2	494·4	994·6	5·8
4	500·2	496·2	996·4	4·0
5	500·2	494·4	994·6	5·8
6	500·2	492·6	992·8	7·6
7	500·0	496·4	996·4	3·6
8	500·0	496·2	996·2	3·8
9	500·0	494·4	994·4	5·6
10	500·0	492·6	992·6	7·4
11	500·0	490·6	990·6	9·4
12	499·8	496·4	996·2	3·4
13	499·8	496·2	996·0	3·6
14	499·8	494·4	994·2	5·4
15	499·8	492·6	992·4	7·2
16	499·8	490·6	990·4	9·2
17	499·8	488·6	988·4	11·2
18	499·6	496·8	996·4	2·8
19	499·6	496·4	996·0	3·2
20	499·6	496·2	995·8	3·4
21	499·6	494·4	994·0	5·2
22	499·6	492·6	992·2	7·0
23	499·6	490·6	990·2	9·0
24	499·6	488·6	988·2	11·0
25	499·6	486·8	986·4	12·8
26	499·3	497·1	996·4	2·2
27	499·3	496·8	996·1	2·5
28	499·3	496·4	995·7	2·9
29	499·3	496·2	995·5	3·1
30	499·3	494·4	993·7	4·9

PT	A′	B′	P′	D′
31	499·3	492·6	991·9	6·7
32	499·3	490·6	989·9	8·7
33	499·3	488·6	987·9	10·7
34	499·3	486·8	986·1	12·5
35	499·3	486·8	986·1	12·5
36	498·9	497·5	996·4	1·4
37	498·9	497·1	996·0	1·8
38	498·9	496·8	995·7	2·1
39	498·9	496·4	995·3	2·5
40	498·9	496·2	995·1	2·7
41	498·9	494·4	993·5	4·5
42	498·9	492·6	991·5	6·3
43	498·9	490·6	989·5	8·3
44	498·9	488·6	987·5	10·3
45	498·9	486·8	985·7	12·1
46	498·9	486·8	985·7	12·1
47	498·6	497·8	996·4	0·8
48	498·6	497·5	996·1	1·1
49	498·6	497·1	995·7	1·5
50	498·6	496·8	995·4	1·8
51	498·6	496·4	995·0	2·2
52	498·6	496·2	994·8	2·4
53	498·6	494·4	993·0	4·2
54	498·6	492·6	991·2	6·0
55	498·6	490·6	989·2	8·0
56	498·6	488·6	987·2	10·0
57	498·6	486·8	985·4	11·8
58	498·6	486·8	985·4	11·8
59	498·2	498·2	996·4	0·0
60	498·2	497·8	996·0	0·4

PT	A′	B′	P′	D′
61	498·2	497·5	995·7	0·7
62	498·2	497·1	995·3	1·1
63	498·2	496·8	995·0	1·4
64	498·2	496·4	994·6	1·8
65	498·2	496·2	994·4	2·0
66	498·2	494·4	992·6	3·8
67	498·2	492·6	990·8	5·6
68	498·2	490·6	988·8	7·6
69	498·2	488·6	986·8	9·6
70	498·2	486·8	985·0	11·4
71	498·2	486·8	985·0	11·4
72	497·8	497·8	995·6	0·0
73	497·8	497·5	995·3	0·3
74	497·8	497·1	994·9	0·7
75	497·8	496·8	994·6	1·0
76	497·8	496·4	994·2	1·4
77	497·8	496·2	994·0	1·6
78	497·8	494·4	992·2	3·4
79	497·8	492·6	990·4	5·2
80	497·8	490·6	988·4	7·2
81	497·8	488·6	986·4	9·2
82	497·8	486·8	984·6	11·0
83	497·8	486·8	984·6	11·0
84	497·5	497·5	995·0	0·0
85	497·5	497·1	994·6	0·4
86	497·5	496·8	994·3	0·7
87	497·5	496·4	993·9	1·1
88	497·5	496·2	993·7	1·3
89	497·5	494·4	991·9	3·1
90	497·5	492·6	990·1	4·9

PT	A′	B′	P′	D′
91	497·5	490·6	988·1	6·9
92	497·5	488·6	986·1	8·9
93	497·5	486·8	984·3	10·7
94	497·5	486·8	984·3	10·7
95	497·1	497·1	994·2	0·0
96	497·1	496·8	993·9	0·3
97	497·1	496·4	993·5	0·7
98	497·1	496·2	993·3	0·9
99	497·1	494·4	991·5	2·7
100	497·1	492·6	9897	4·5
101	497·1	490·6	987·7	6·5
102	497·1	488·6	985·7	8·5
103	497·1	486·8	983·9	10·3
104	497·1	486·8	983·9	10·3
105	496·8	496·8	993·6	0·0
106	496·8	496·4	993·2	0·4
107	496·8	496·2	993·0	0·6
108	496·8	494·4	991·2	2·4
109	496·8	492·6	989·4	4·2
110	496·8	490·6	987·4	6·2
111	496·8	488·6	985·4	8·2
112	496·8	486·8	983·6	10·0
113	496·8	486·8	983·6	10·0
114	496·4	496·4	992·8	0·0
115	496·4	496·2	992·6	0·2
116	496·4	494·4	990·8	2·0
117	496·4	492·6	989·0	3·8
118	496·4	490·6	987·0	5·8
119	496·4	488·6	985·0	7·8
120	496·4	486·8	983·2	9·6

PT	A′	B′	P′	D′
121	496·4	486·8	983·2	9·6
122	496·2	496·2	992·4	0·0
123	496·2	494·4	990·6	1·8
124	496·2	492·6	988·8	3·6
125	496·2	490·6	986·8	5·6
126	496·2	488·6	984·8	7·6
127	496·2	486·8	983·0	9·4
128	496·2	486·8	983·0	9·4
129	494·4	494·4	988·8	0·0
130	494·4	492·6	987·0	1·8
131	494·4	490·6	985·0	3·8
132	494·4	488·6	983·0	5·8
133	494·4	486·8	981·2	7·6
134	494·4	486·8	981·2	7·6
135	492·6	492·6	985·2	0·0
136	492·6	490·6	983·2	2·0
137	492·6	488·6	981·2	4·0
138	492·6	486·8	979·4	5·8
139	492·6	486·8	979·4	5·8
140	490·6	490·6	981·2	0·0
141	490·6	488·6	979·2	2·0
142	490·6	486·8	977·4	3·8
143	490·6	486·8	977·4	3·8
144	488·6	488·6	977·2	0·0
145	488·6	486·8	975·4	1·8
146	488·6	486·8	975·4	1·8
147	486·8	486·8	973·6	0·0
148	486·8	486·8	973·6	0·0

FIG. 3. Design for Mach number 2·00 nozzle.

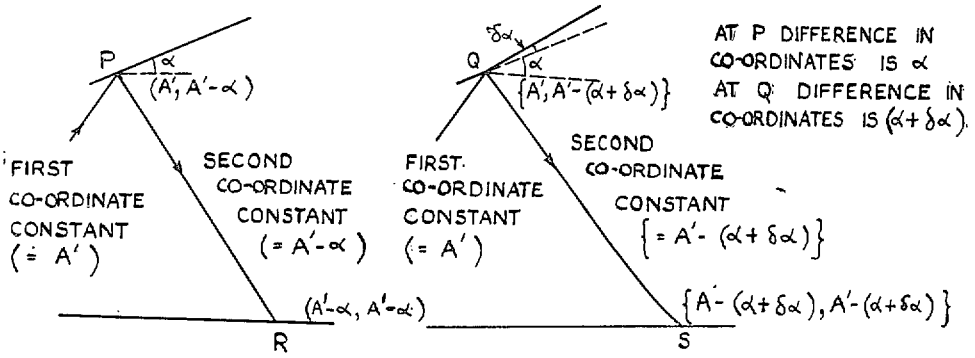

FIG. 4. Effect of change in wall inclination method for re-design of nozzles.

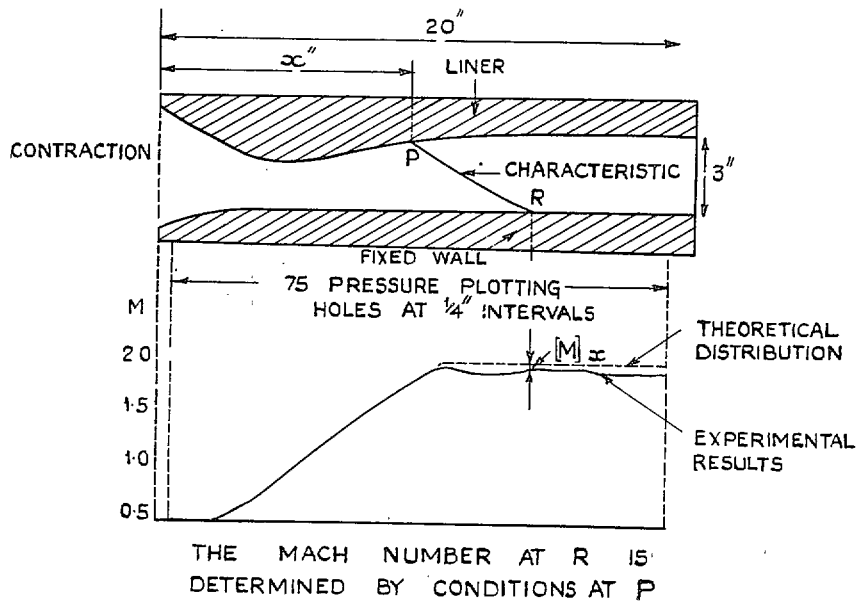

FIG. 5. Diagram illustrating x and $[M]_x$ method for re-design of nozzles.

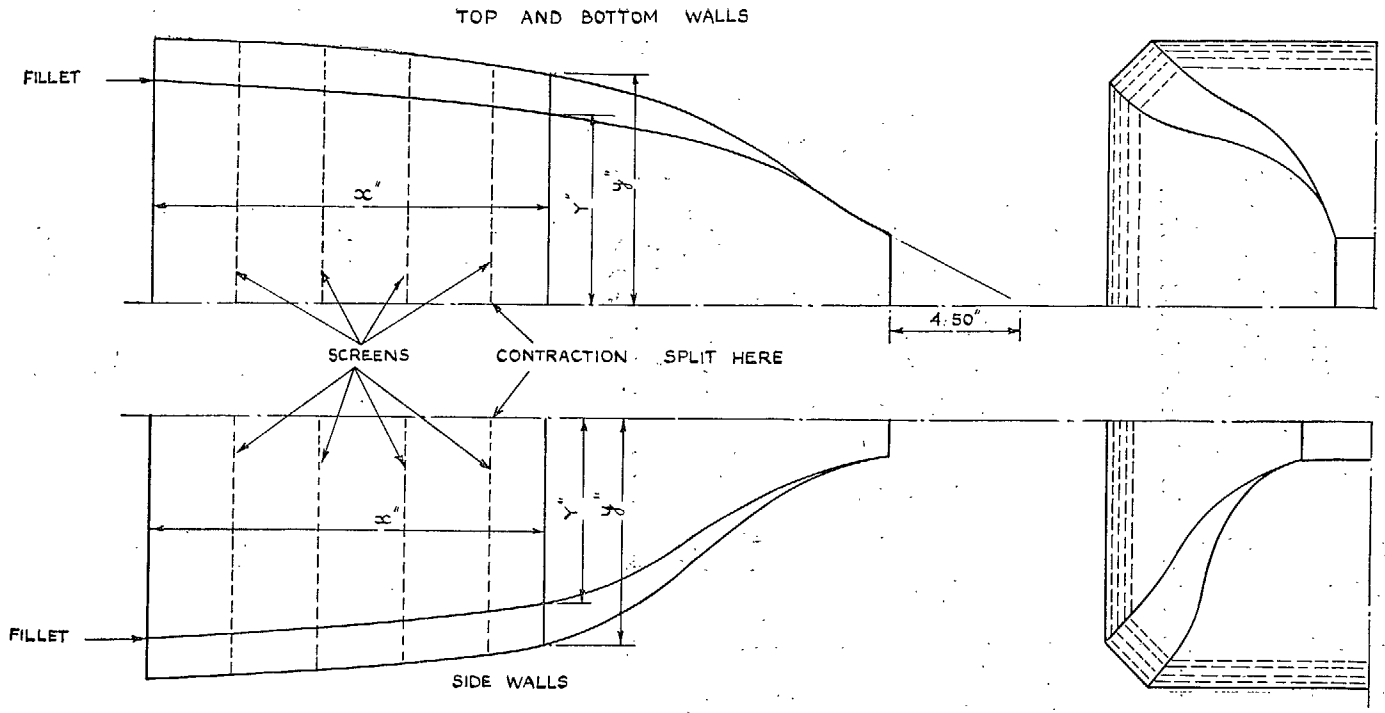

TOP AND BOTTOM WALLS.

x IN.	WALL y IN.	FILLET Y IN.
0	9·25	7·75
2·0	9·14	7·64
4·0	9·01	7·51
6·0	8·91	7·41
8·0	8·75	7·25
10·0	8·56	7·06
12·0	8·30	6·81
14·0	7·99	6·58
16·0	7·58	6·28
18·0	7·01	5·91
20·0	6·21	5·43
22·0	5·04	4·74
24·0	3·61	3·61
26·0	2·42	—

SIDE WALLS

x IN.	WALL y IN.	FILLET Y IN.
0	9·25	7·75
2·0	9·14	7·64
4·0	9·01	7·51
6·0	8·91	7·41
8·0	8·75	7·25
10·0	8·56	7·06
12·0	8·30	6·81
14·0	7·92	6·51
16·0	7·24	5·94
18·0	6·12	5·02
20·0	4·36	3·62
22·0	2·83	2·55
24·0	1·84	1·84
26·0	1·50	—

FIG. 6. Co-ordinates of 3-in. tunnel contraction.

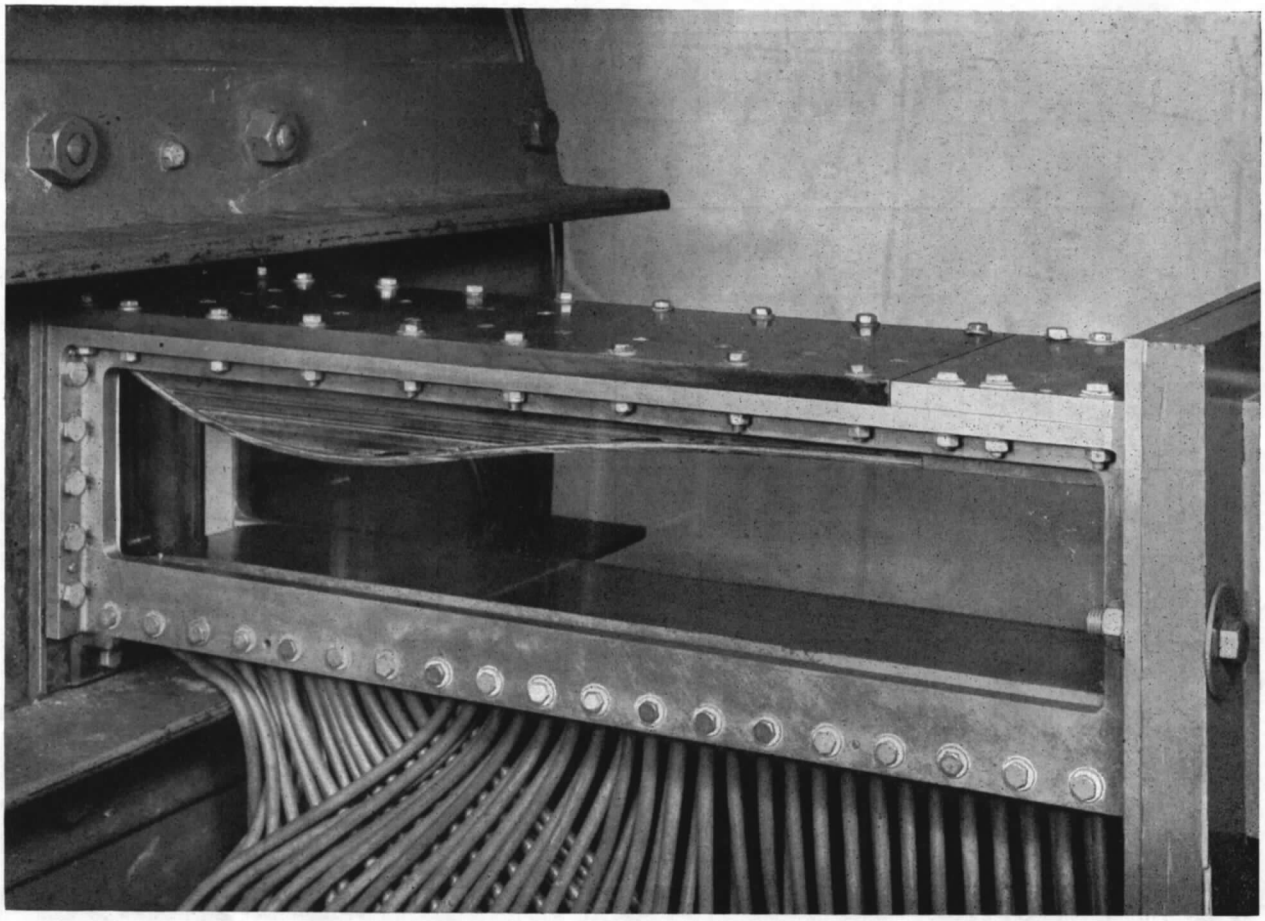

FIG. 7. Working section of 3-in. tunnel.

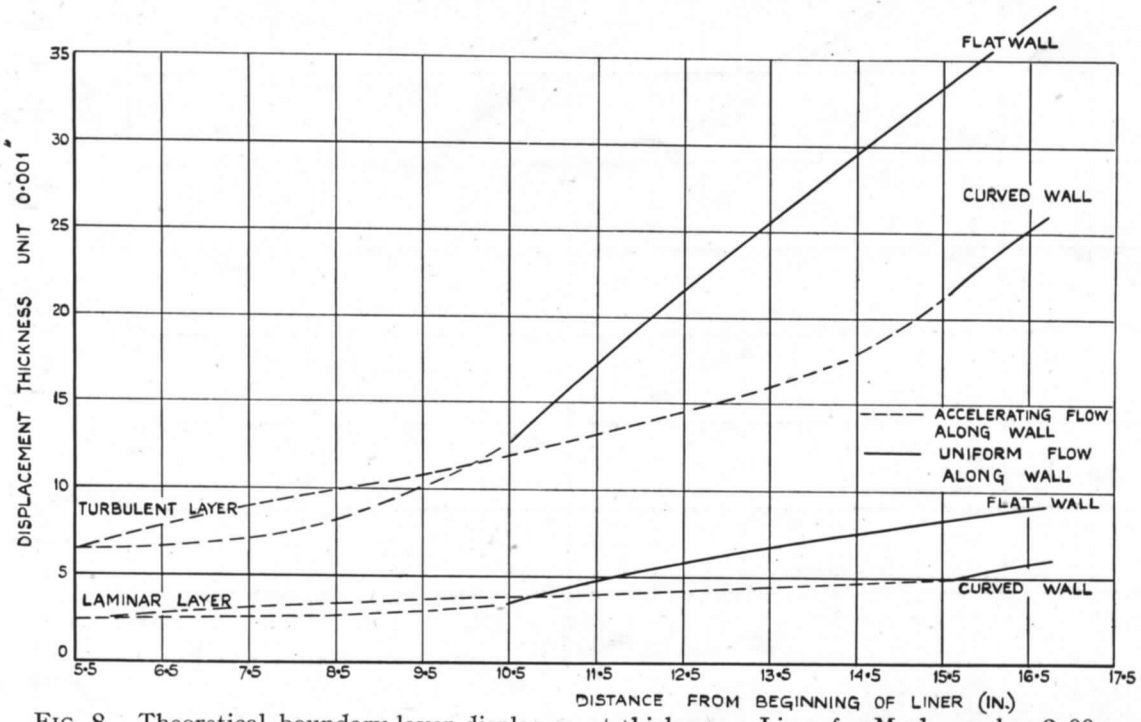

FIG. 8. Theoretical boundary-layer displacement-thickness. Liner for Mach number 2·00.

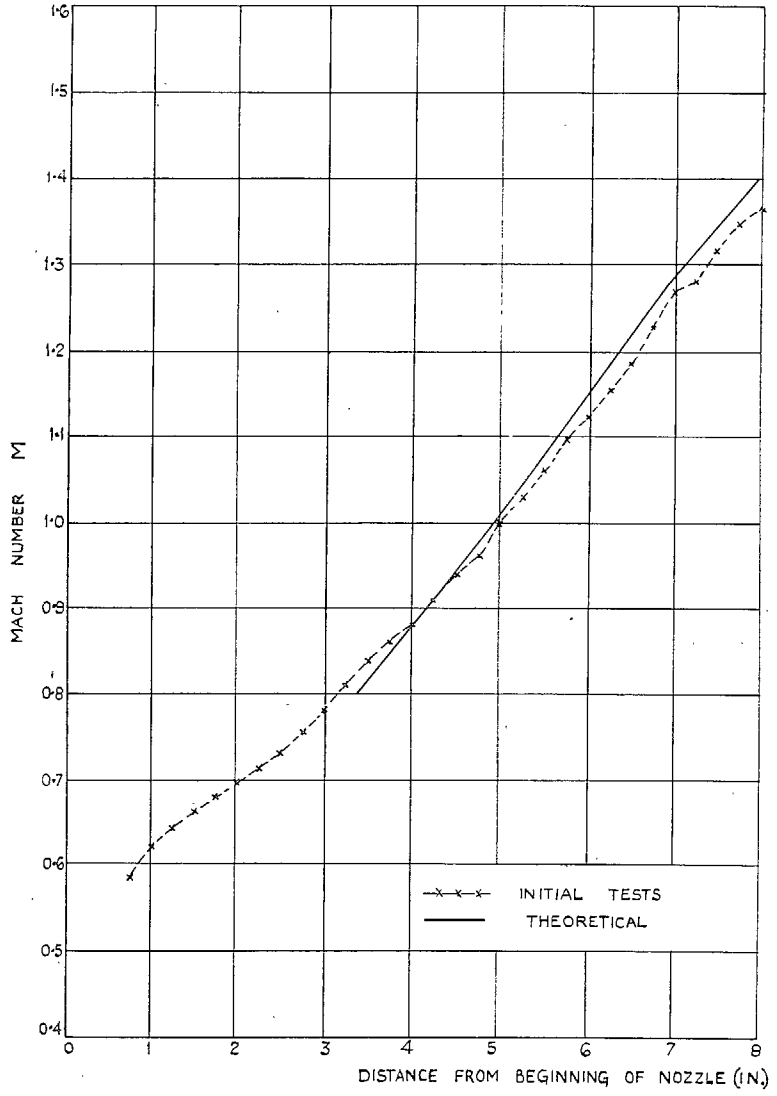

FIG. 9. Original liner for Mach number 1·40.
Mach number distributions. Contraction end.

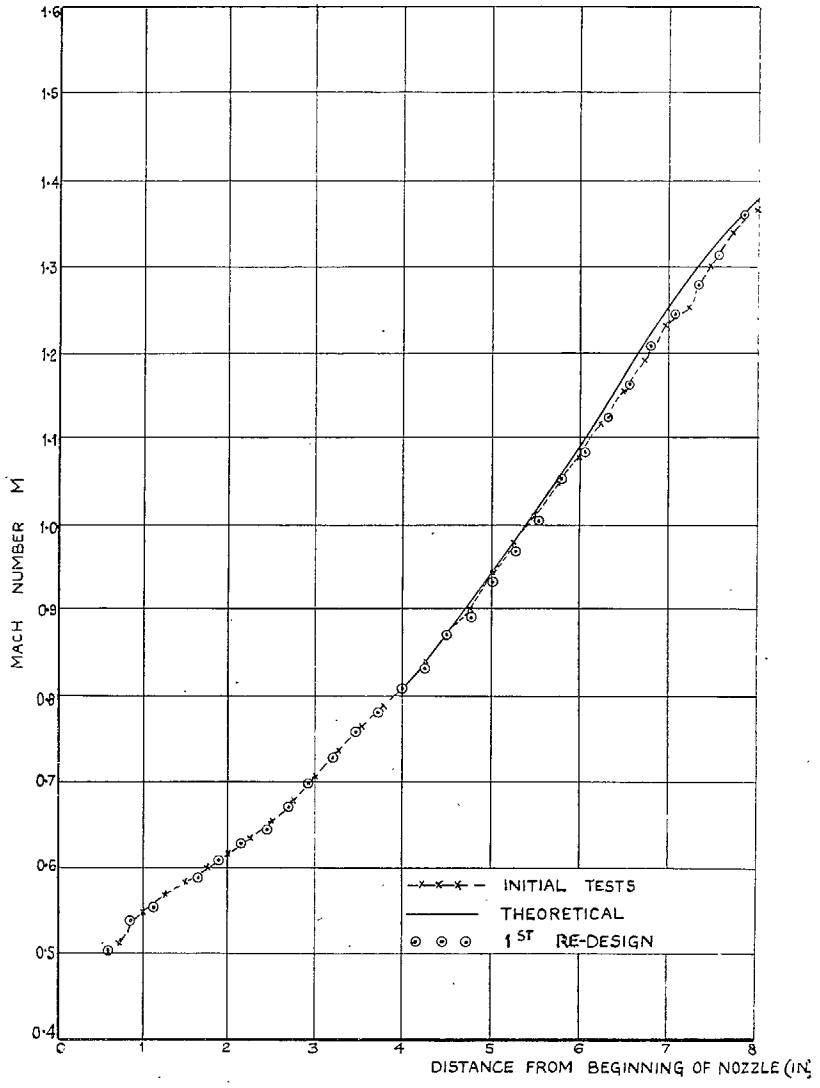

FIG. 10. Original liner for Mach number 1·60.
Mach number distributions. Contraction end.

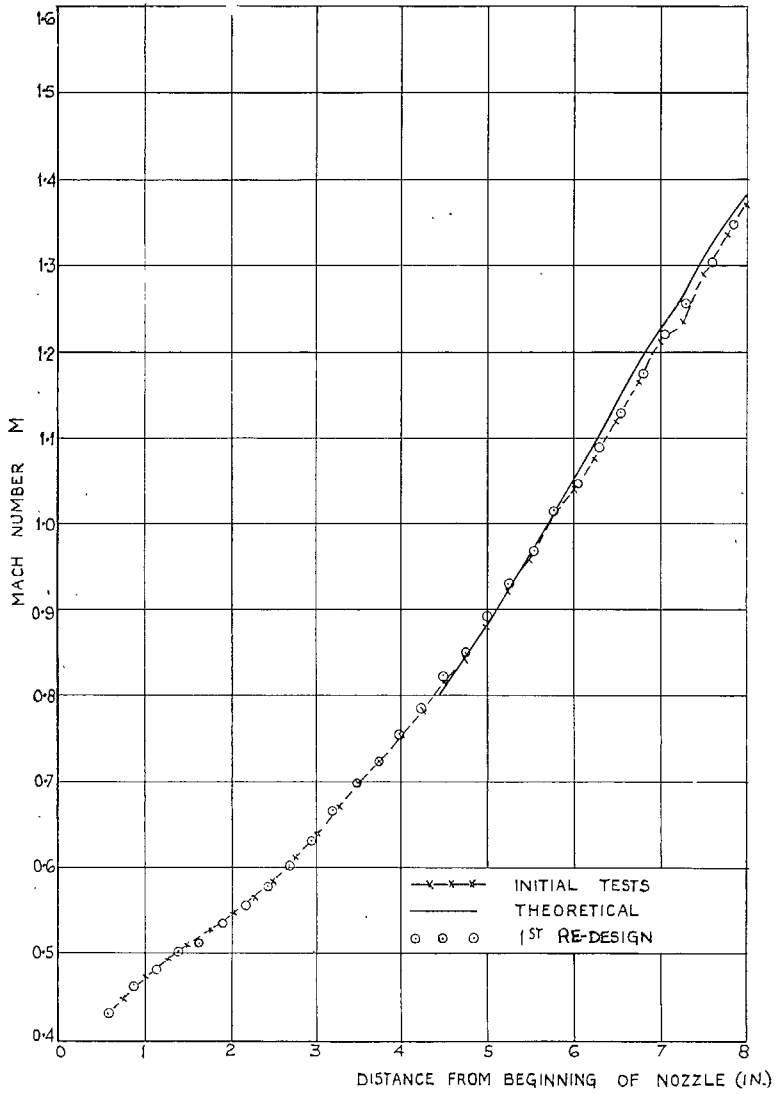

FIG. 11. Original liner for Mach number 1·80.
Mach number distributions. Contraction end.

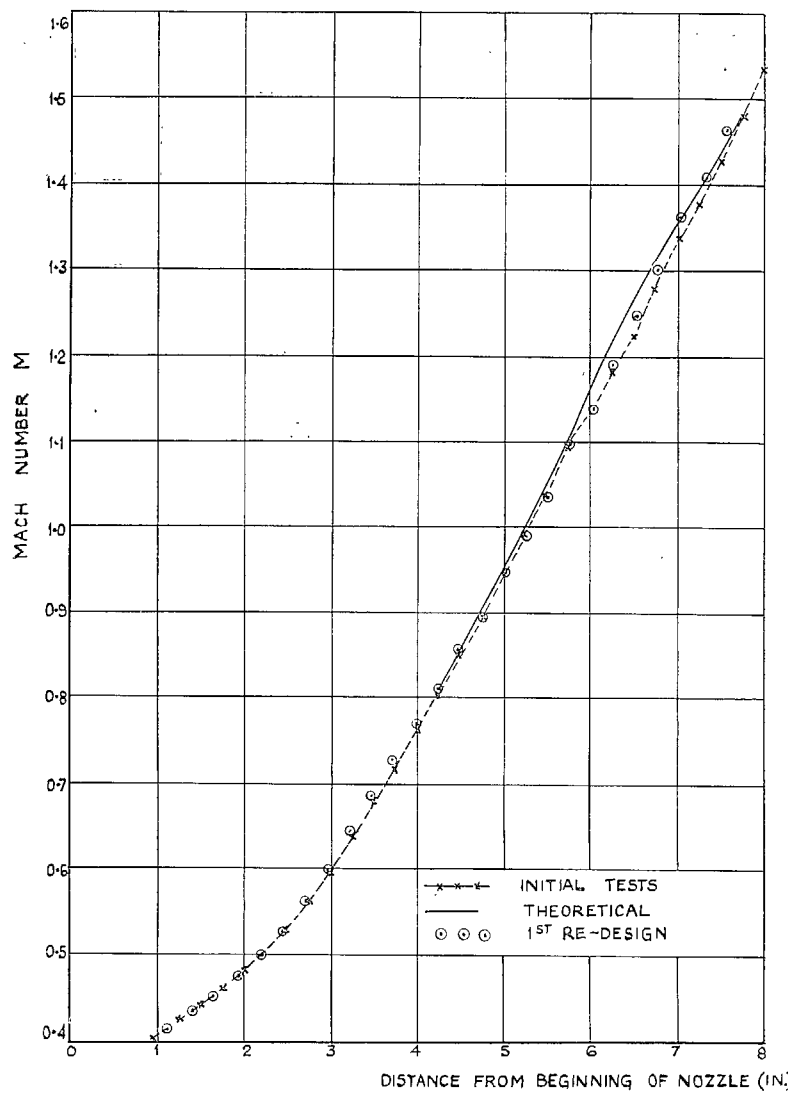

FIG. 12. Original liner for Mach number 2·00.
Mach number distributions. Contraction end.

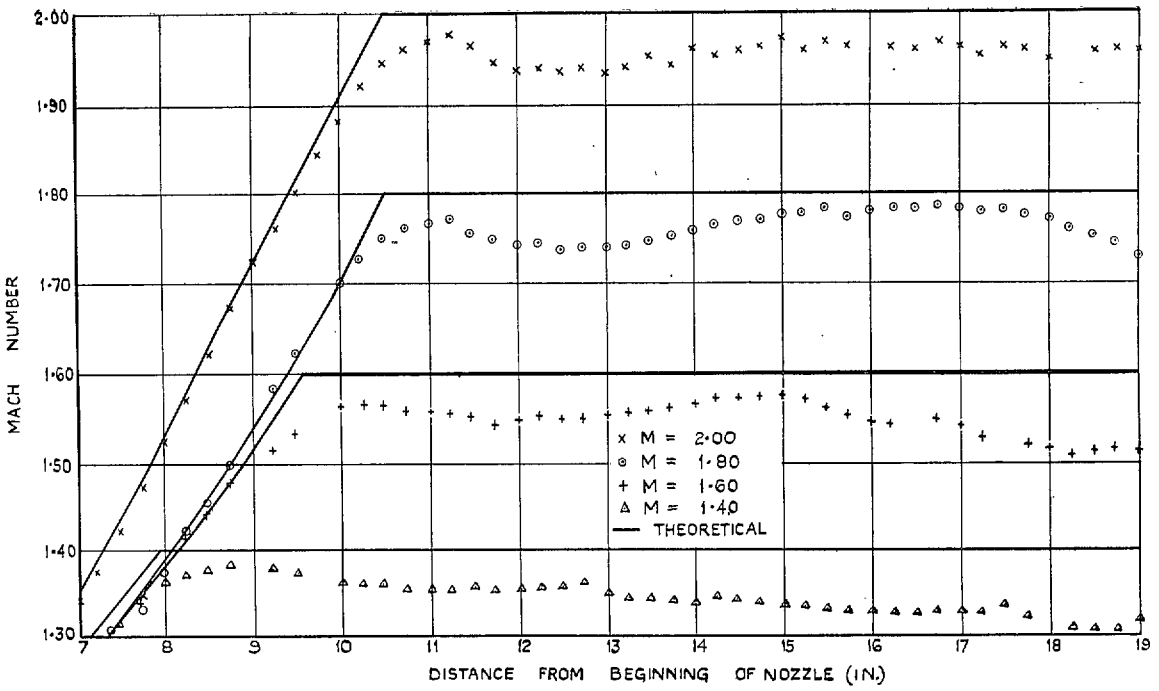

FIG. 13. Mach number distributions. Initial tests on original liners.

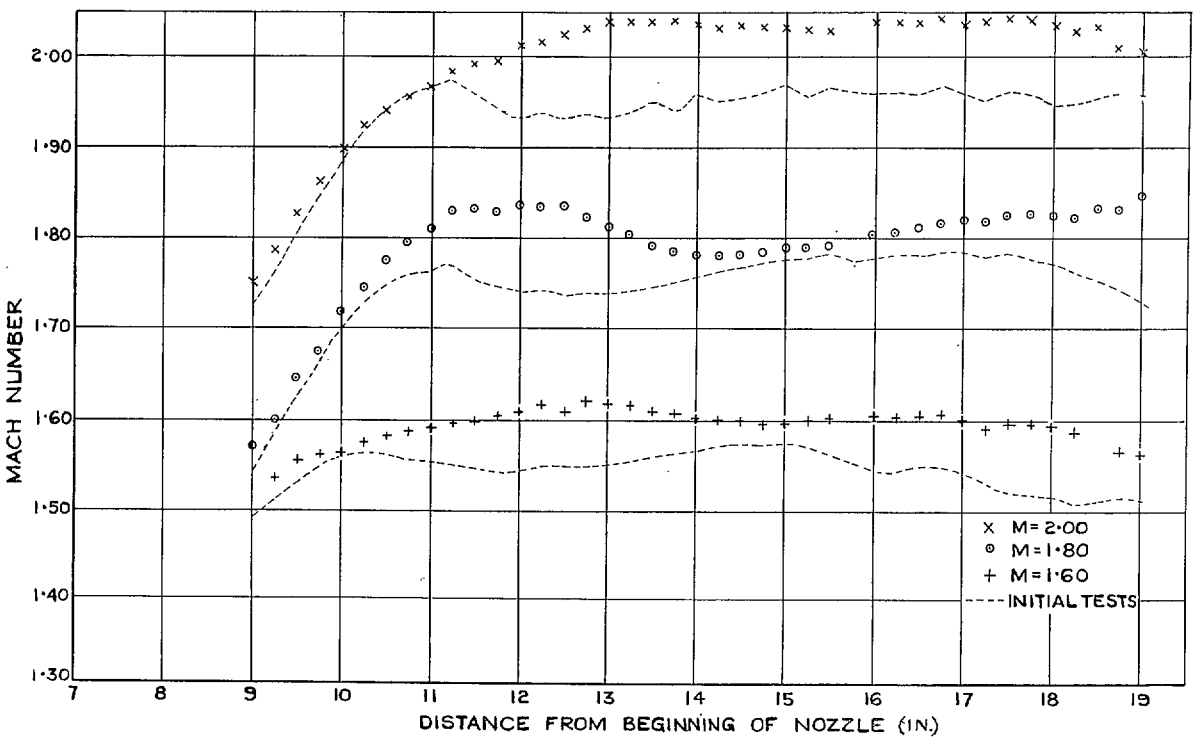

FIG. 14. Mach number distributions. First re-design of original liners.

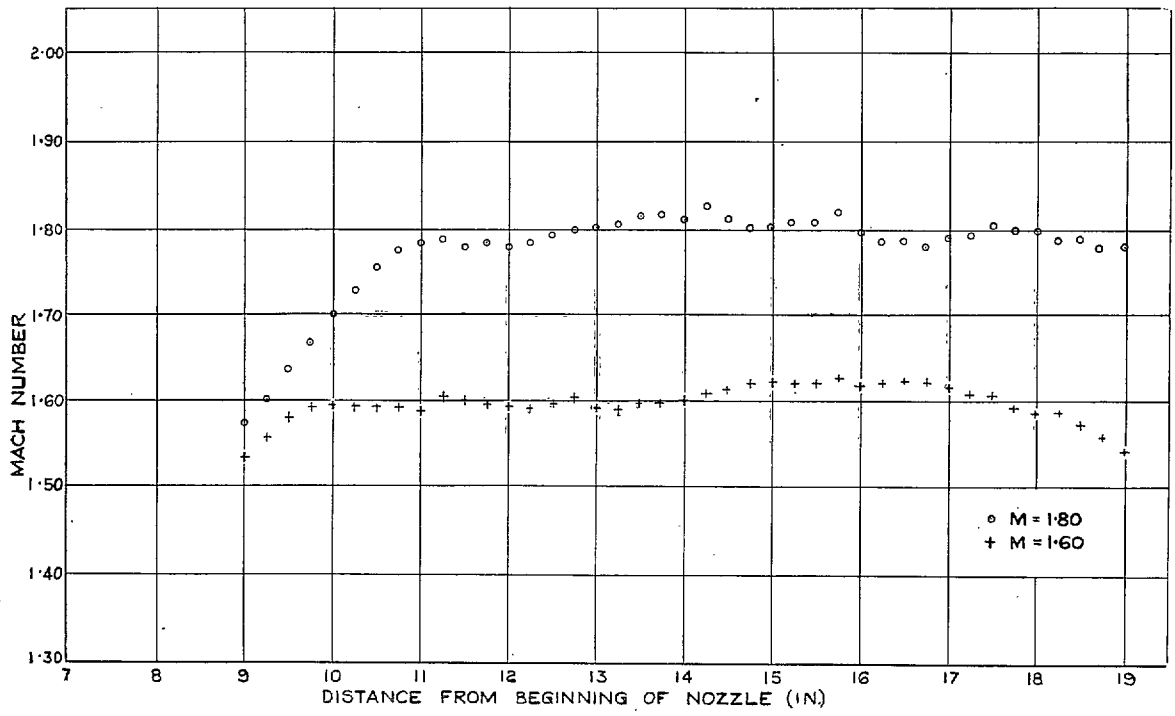

FIG. 15. Mach number distributions. Final tests on original liners.

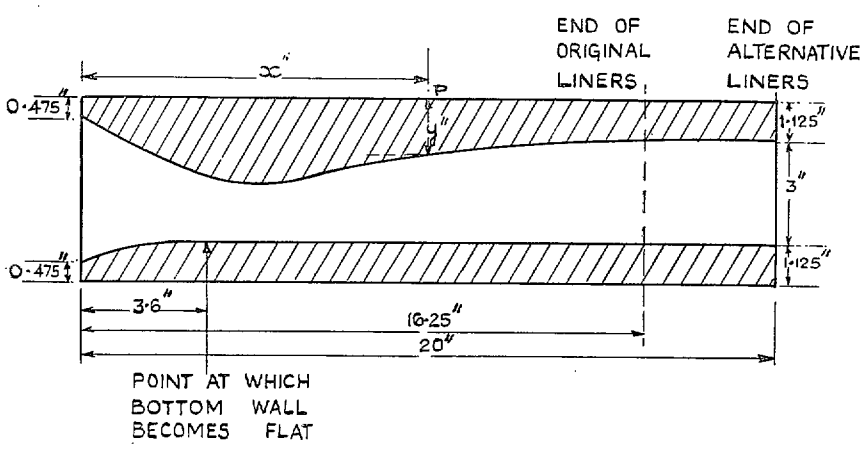

FIG. 16. Measurement of template co-ordinates.

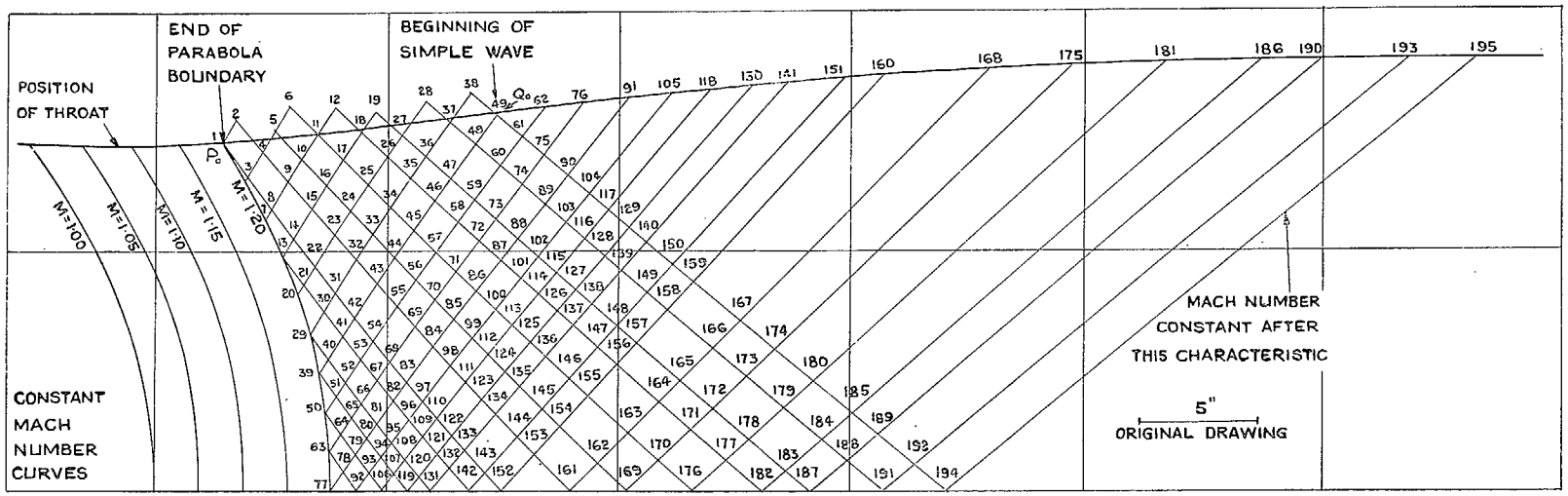

TABLE OF VALUES A' B' P' D'

PT	A'	B'	P'	D'
1	500·2	496·2	996·4	4·0
2	500·2	495·3	995·5	4·9
3	500·2	496·2	996·4	4·0
4	500·2	495·3	995·5	4·9
5	500·2	494·6	994·8	5·6
6	500·2	493·9	994·1	6·3
7	500·2	496·2	996·4	4·0
8	500·2	496·2	996·4	4·0
9	500·2	495·3	995·5	4·9
10	500·2	494·6	994·8	5·6
11	500·2	493·9	994·1	6·3
12	500·2	493·3	993·5	6·9
13	500·0	496·4	996·4	3·6
14	500·0	496·2	996·2	3·8
15	500·0	495·3	995·3	4·7
16	500·0	494·6	994·6	5·4
17	500·0	493·9	993·9	6·1
18	500·0	493·3	993·3	6·7
19	500·0	493·0	993·0	7·0
20	499·8	496·6	996·4	3·2
21	499·8	496·4	996·2	3·4
22	499·8	496·2	996·0	3·6
23	499·8	495·3	995·1	4·5
24	499·8	494·6	994·4	5·2
25	499·8	493·9	993·7	5·9
26	499·8	493·3	993·1	6·5
27	499·8	493·0	992·8	6·8
28	499·8	492·7	992·5	7·1
29	499·6	496·8	996·4	2·8
30	499·6	496·4	996·0	3·2
31	499·6	496·2	995·8	3·4
32	499·6	495·3	994·9	4·3
33	499·6	494·6	994·2	5·0
34	499·6	493·9	993·5	5·7
35	499·6	493·3	992·9	6·3
36	499·6	493·0	992·6	6·6
37	499·6	492·7	992·3	6·9
38	499·6	492·6	992·2	7·0
39	499·3	497·1	996·4	2·2
40	499·3	496·8	996·1	2·5
41	499·3	496·4	995·7	2·9
42	499·3	496·2	995·5	3·1
43	499·3	495·3	994·6	4·0
44	499·3	494·6	993·9	4·7
45	499·3	493·9	993·2	5·4
46	499·3	493·3	992·6	6·0
47	499·3	493·0	992·3	6·3
48	499·3	492·7	992·0	6·6
49	499·3	492·6	991·9	6·7
50	498·9	497·5	996·4	1·4
51	498·9	497·1	996·0	1·8
52	498·9	496·8	995·7	2·1
53	498·9	496·4	995·3	2·5
54	498·9	496·2	995·1	2·7
55	498·9	495·3	994·2	3·6
56	498·9	494·6	993·5	4·3
57	498·9	493·9	992·8	5·0
58	498·9	493·3	992·2	5·6
59	498·9	493·0	991·9	5·9
60	498·9	492·7	991·6	6·2
61	498·9	492·6	991·5	6·3
62	498·9	492·6	991·5	6·3
63	498·6	497·8	996·4	0·8
64	498·6	497·5	996·1	1·1
65	498·6	497·1	995·7	1·5
66	498·6	496·8	995·4	1·8
67	498·6	496·4	995·0	2·2
68	498·6	496·2	994·8	2·4
69	498·6	495·3	993·9	3·3
70	498·6	494·6	993·2	4·0
71	498·6	493·9	992·5	4·7
72	498·6	493·3	991·9	5·3
73	498·6	493·0	991·6	5·6
74	498·6	492·7	991·3	5·9
75	498·6	492·6	991·2	6·0
76	498·6	492·6	991·2	6·0
77	498·2	498·2	996·4	0·0
78	498·2	497·8	996·0	0·4
79	498·2	497·5	995·7	0·7
80	498·2	497·1	995·3	1·1
81	498·2	496·8	995·0	1·4
82	498·2	496·4	994·6	1·8
83	498·2	496·2	994·4	2·0
84	498·2	495·3	993·5	2·9
85	498·2	494·6	992·8	3·6
86	498·2	493·9	992·1	4·3
87	498·2	493·3	991·5	4·9
88	498·2	493·0	991·2	5·2
89	498·2	492·7	990·9	5·5
90	498·2	492·6	990·8	5·6
91	498·2	492·6	990·8	5·6
92	497·8	497·8	995·6	0·0
93	497·8	497·5	995·3	0·3
94	497·8	497·1	994·9	0·7
95	497·8	496·8	994·6	1·0
96	497·8	496·4	994·2	1·4
97	497·8	496·2	994·0	1·6
98	497·8	495·3	993·1	2·5
99	497·8	494·6	992·4	3·2
100	497·8	493·9	991·7	3·9
101	497·8	493·3	991·1	4·5
102	497·8	493·0	990·8	4·8
103	497·8	492·7	990·5	5·1
104	497·8	492·6	990·4	5·2
105	497·8	492·6	990·4	5·2
106	497·5	497·5	995·0	0·0
107	497·5	497·1	994·6	0·4
108	497·5	496·8	994·3	0·7
109	497·5	496·4	993·9	1·1
110	497·5	496·2	993·7	1·3
111	497·5	495·3	992·8	2·2
112	497·5	494·6	992·1	2·9
113	497·5	493·9	991·4	3·6
114	497·5	493·3	990·8	4·2
115	497·5	493·0	990·5	4·5
116	497·5	492·7	990·2	4·8
117	497·5	492·6	990·1	4·9
118	497·5	492·6	990·1	4·9
119	497·1	497·1	994·2	0·0
120	497·1	496·8	993·9	0·3
121	497·1	496·4	993·5	0·7
122	497·1	496·2	993·3	0·9
123	497·1	495·3	992·4	1·8
124	497·1	494·6	991·7	2·5
125	497·1	493·9	991·0	3·2
126	497·1	493·3	990·4	3·8
127	497·1	493·0	990·1	4·1
128	497·1	492·7	989·8	4·4
129	497·1	492·6	989·7	4·5
130	497·1	492·6	989·7	4·5
131	496·8	496·8	993·6	0·0
132	496·8	496·4	993·2	0·4
133	496·8	496·2	993·0	0·6
134	496·8	495·3	992·1	1·5
135	496·8	494·6	991·4	2·2
136	496·8	493·9	990·7	2·9
137	496·8	493·3	990·1	3·5
138	496·8	493·0	989·8	3·8
139	496·8	492·7	989·5	4·1
140	496·8	492·6	989·4	4·2
141	496·8	492·6	989·4	4·2
142	496·4	496·4	992·8	0·0
143	496·4	496·2	992·6	0·2
144	496·4	495·3	991·7	1·1
145	496·4	494·6	991·0	1·8
146	496·4	493·9	990·3	2·5
147	496·4	493·3	989·7	3·1
148	496·4	493·0	989·4	3·4
149	496·4	492·7	989·1	3·7
150	496·4	492·6	989·0	3·8
151	496·4	492·6	989·0	3·8
152	496·2	496·2	992·4	0·0
153	496·2	495·3	991·5	0·9
154	496·2	494·6	990·8	1·6
155	496·2	493·9	990·1	2·3
156	496·2	493·3	989·5	2·9
157	496·2	493·0	989·2	3·2
158	496·2	492·7	988·9	3·5
159	496·2	492·6	988·8	3·6
160	496·2	492·6	988·8	3·6
161	495·3	495·3	990·6	0·0
162	495·3	494·6	989·9	0·7
163	495·3	493·9	989·2	1·4
164	495·3	493·3	988·6	2·0
165	495·3	493·0	988·3	2·3
166	495·3	492·7	988·0	2·6
167	495·3	492·6	987·9	2·7
168	495·3	492·6	987·9	2·7
169	494·6	494·6	989·2	0·0
170	494·6	493·9	988·5	0·7
171	494·6	493·3	987·9	1·3
172	494·6	493·0	987·6	1·6
173	494·6	492·7	987·3	1·9
174	494·6	492·6	987·2	2·0
175	494·6	492·6	987·2	2·0
176	493·9	493·9	987·8	0·0
177	493·9	493·3	987·2	0·6
178	493·9	493·0	986·9	0·9
179	493·9	492·7	986·6	1·2
180	493·9	492·6	986·5	1·3
181	493·9	492·6	986·5	1·3
182	493·3	493·3	986·6	0·0
183	493·3	493·0	986·3	0·3
184	493·3	492·7	986·0	0·6
185	493·3	492·6	985·9	0·7
186	493·3	492·6	985·9	0·7
187	493·0	493·0	986·0	0·0
188	493·0	492·7	985·7	0·3
189	493·0	492·6	985·6	0·4
190	493·0	492·6	985·6	0·4
191	492·7	492·7	985·4	0·0
192	492·7	492·6	985·3	0·1
193	492·7	492·6	985·3	0·1
194	492·6	492·6	985·2	0·0
195	492·6	492·6	985·2	0·0

FIG. 17. Alternative design for Mach number 1·60 nozzle.

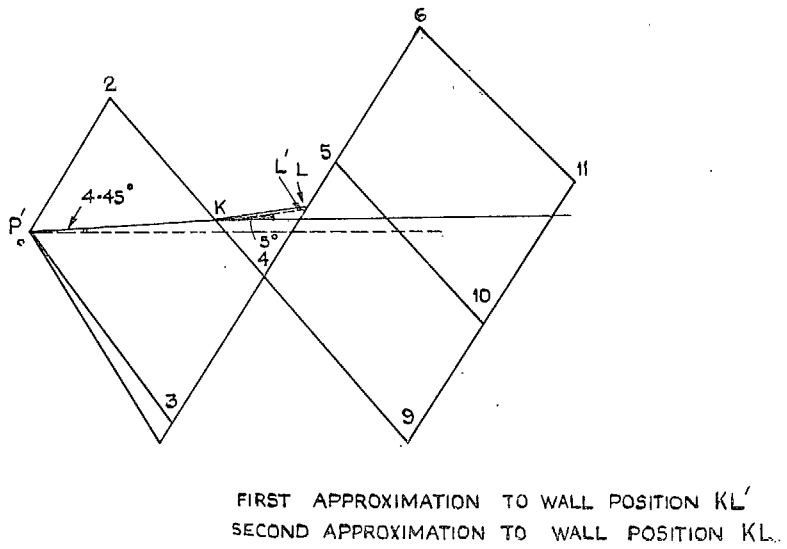

FIG. 18. Construction of wall. Alternative liners.

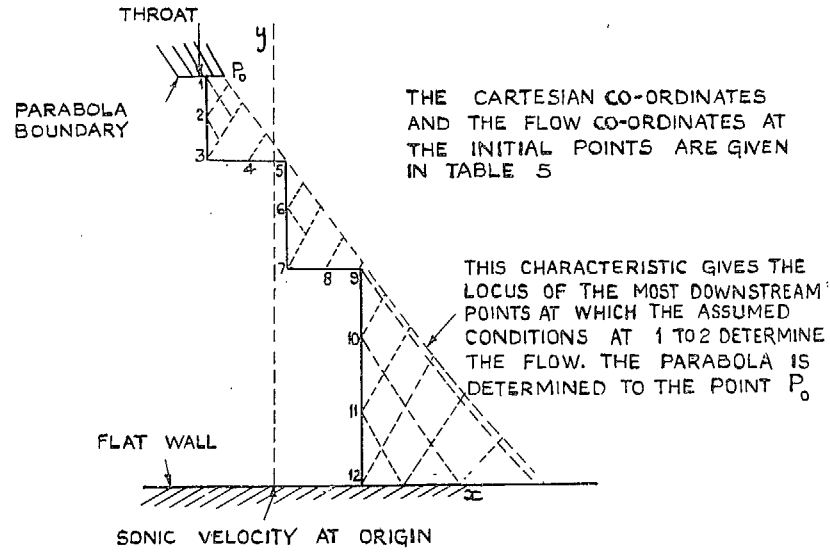

FIG. 19. Alternative initial points for the method of characteristics.

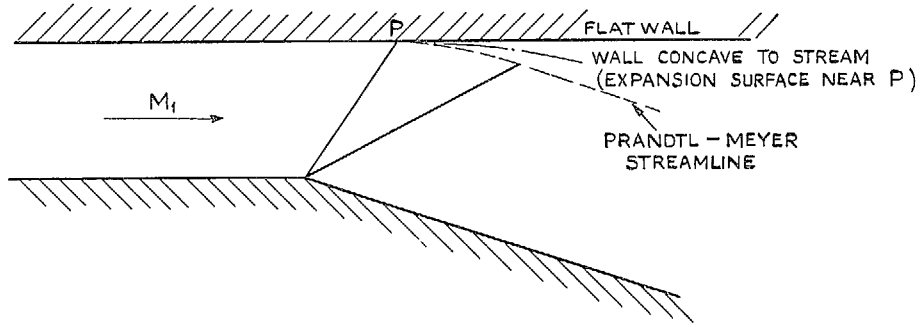

FIG. 20. Expansion from a concave surface.

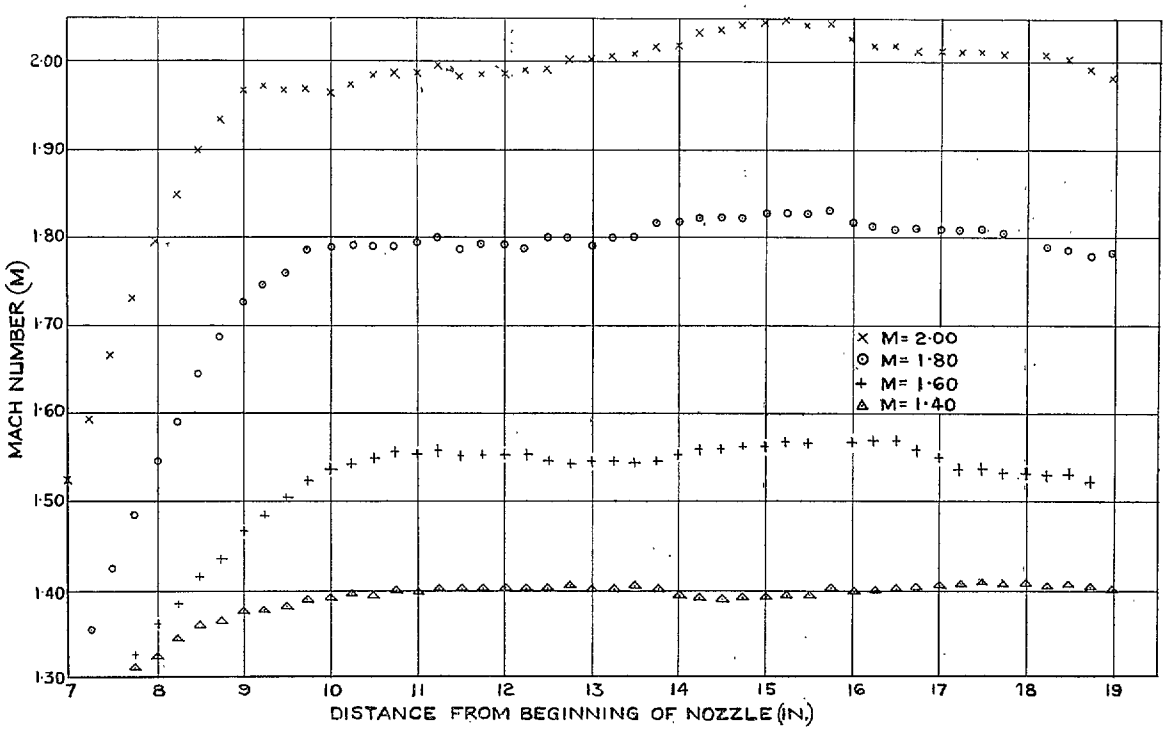

FIG. 21. Mach number distributions. Initial tests on alternative liners.

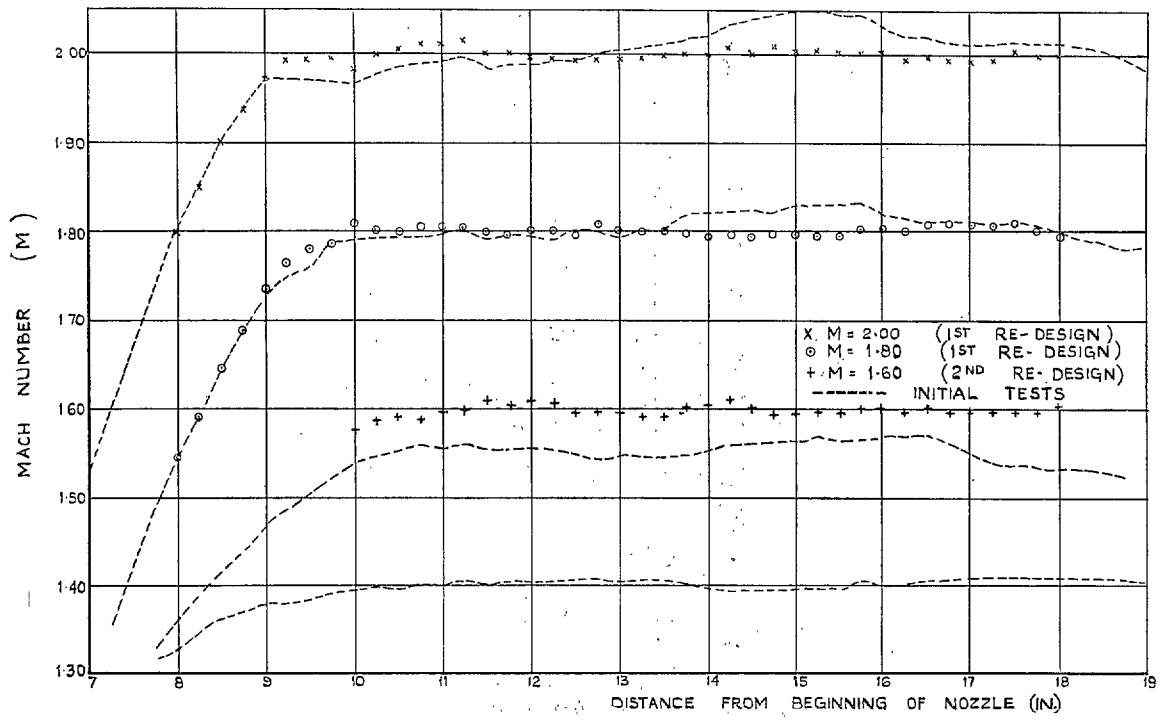

FIG. 22. Mach number distributions. Final tests on alternative liners.

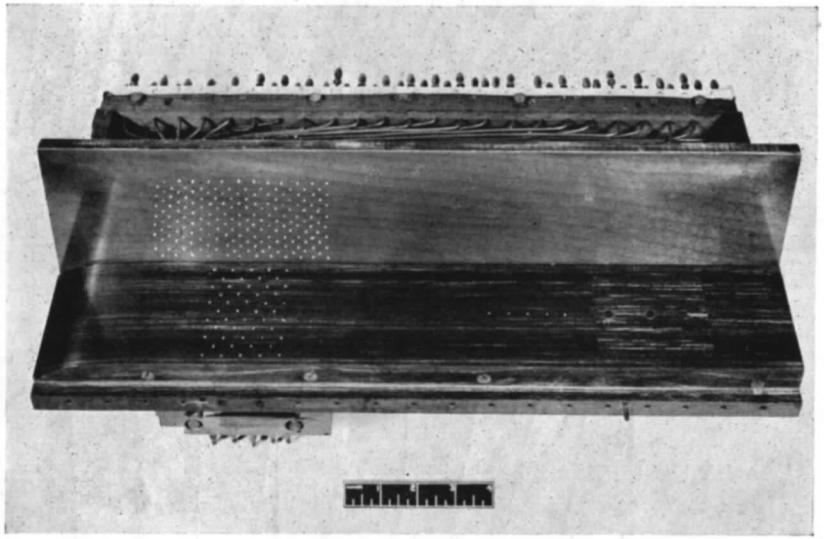

FIG. 23. Arrangement of pressure-plotting walls.

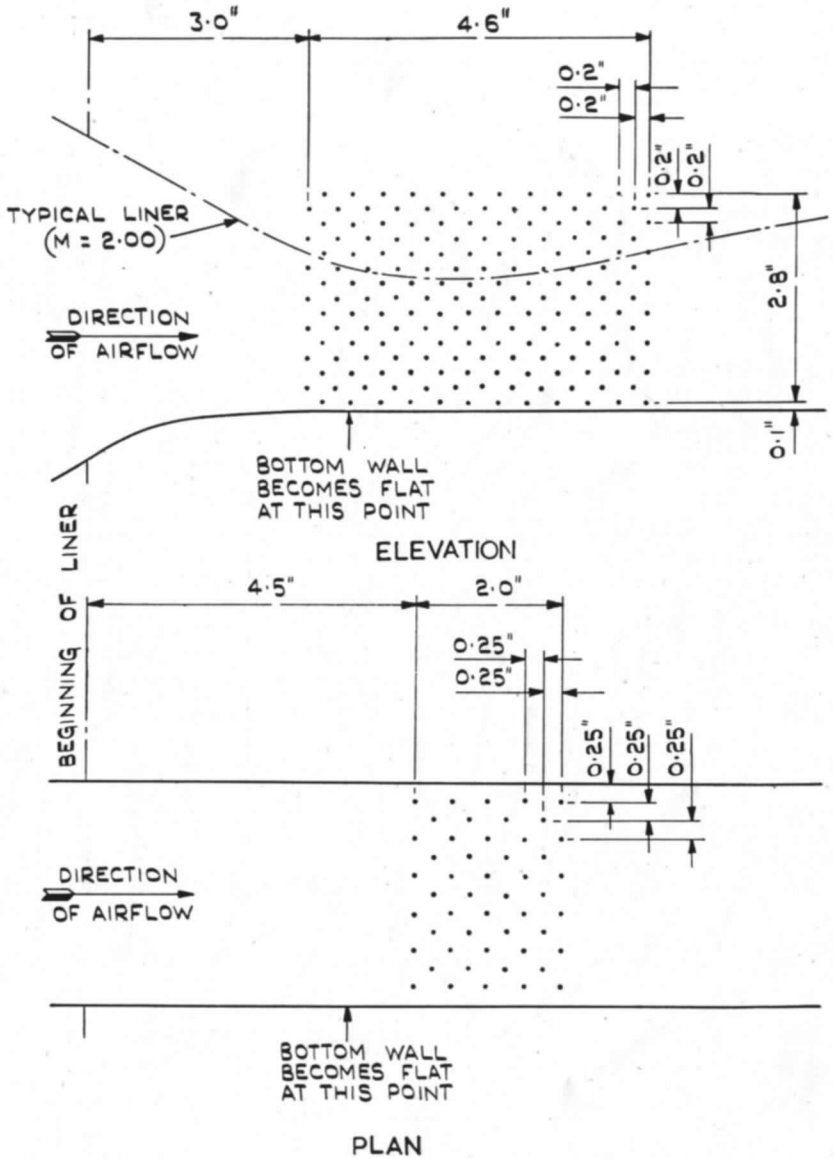

FIG. 24. Position of static holes on side and bottom walls.

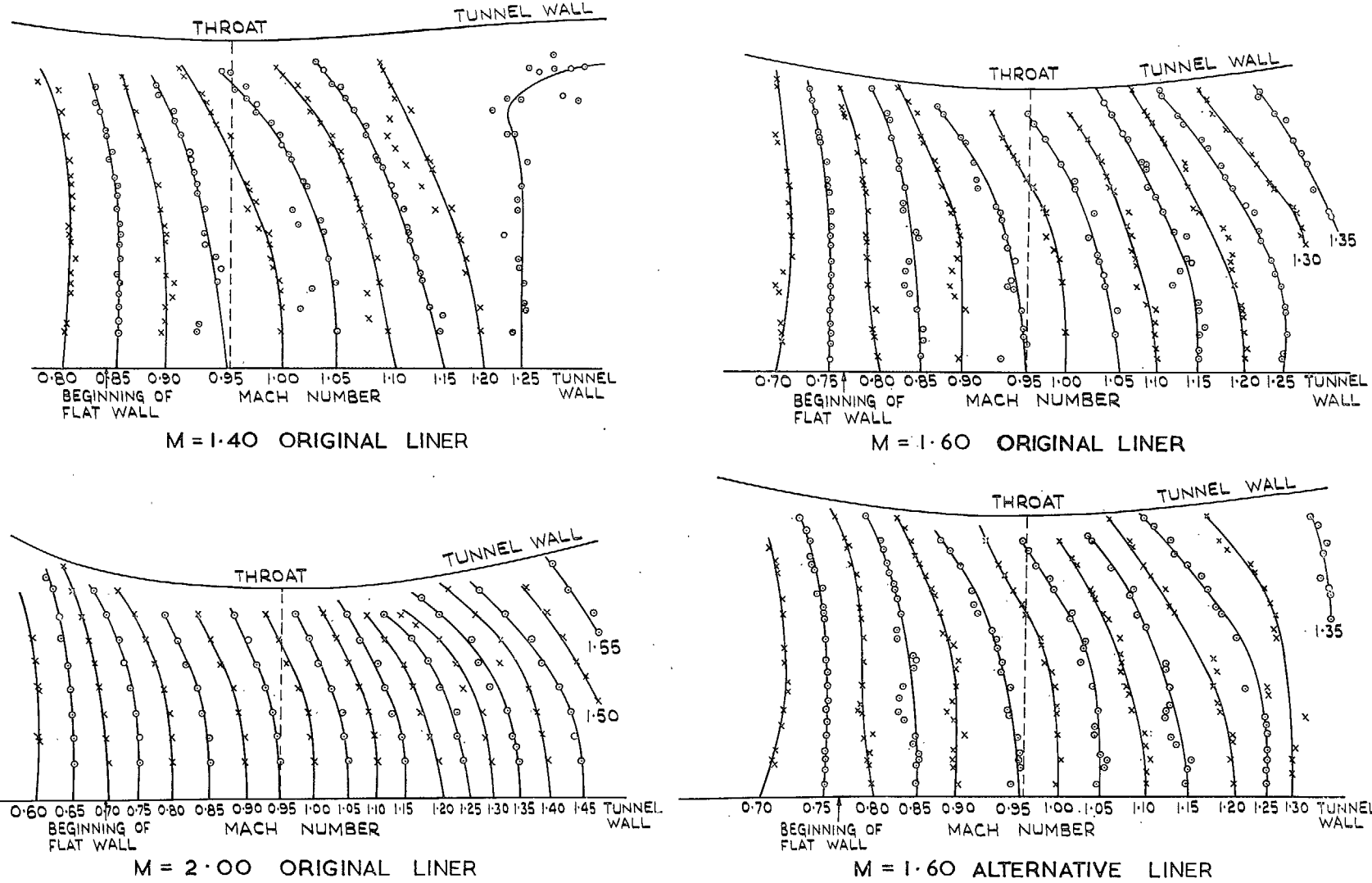

FIG. 25. Flow through a sonic throat. Experimental results.

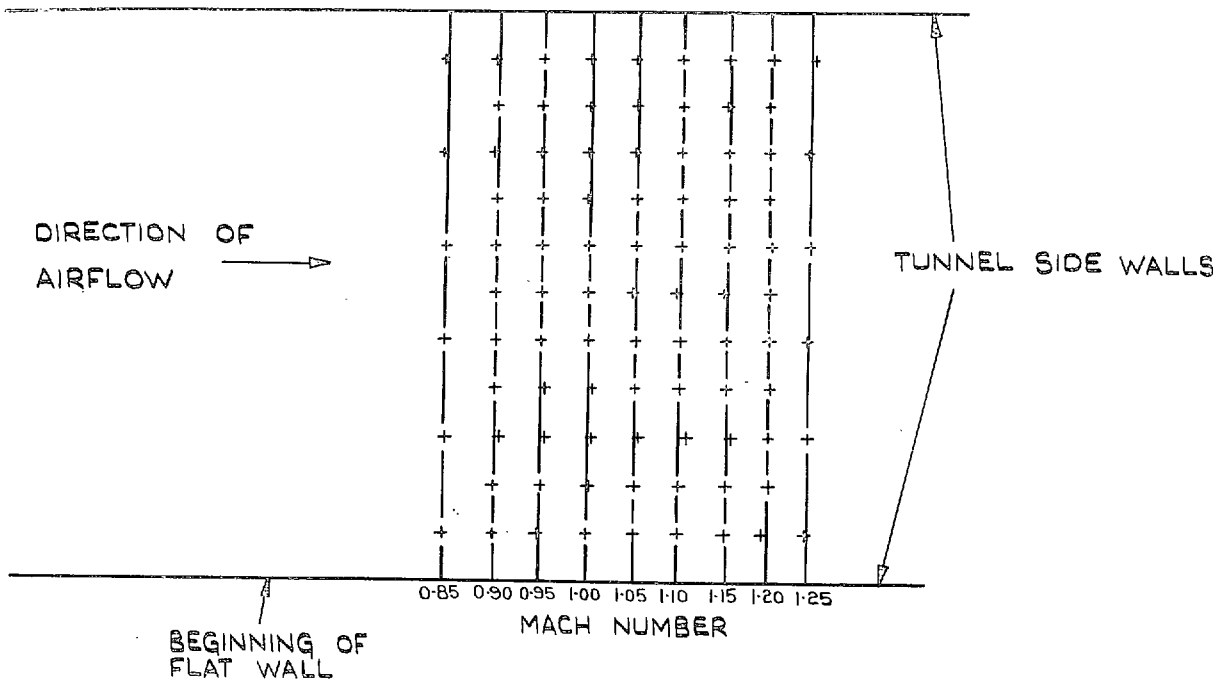

FIG. 26. Flow through a sonic throat. Mach number distribution over bottom wall. Liner for Mach number 2·00.

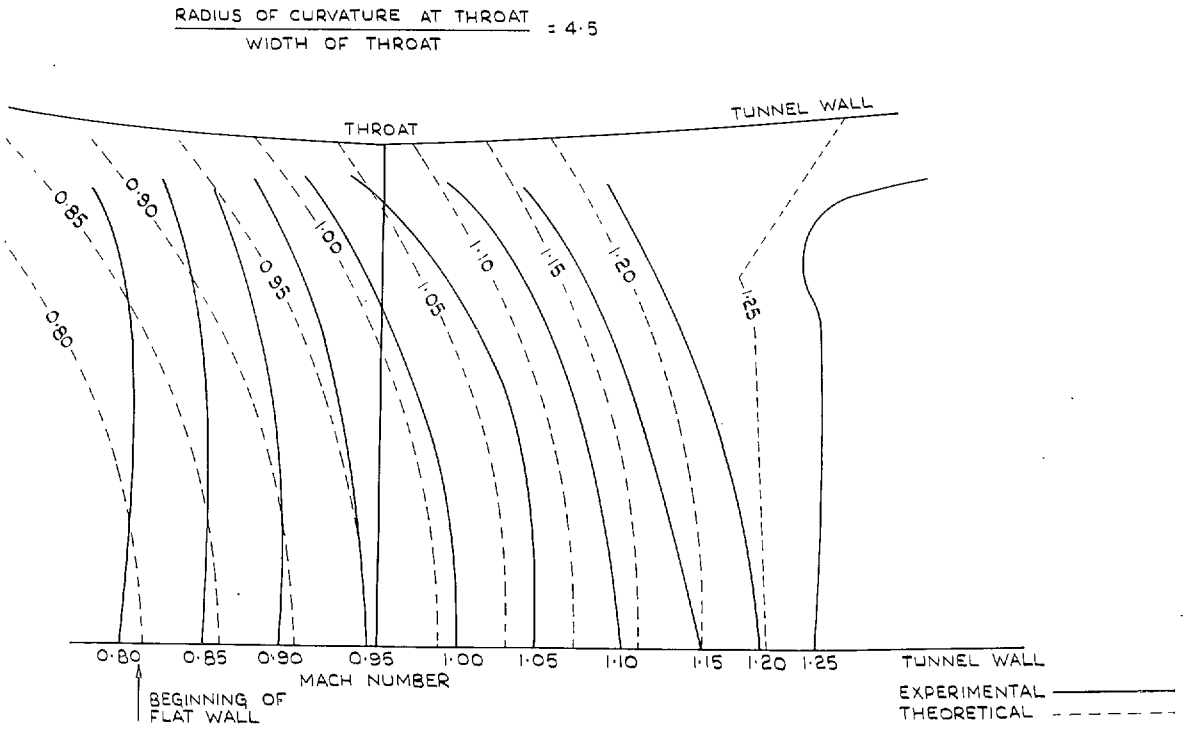

FIG. 27. Flow through a sonic throat. Comparison of theoretical and experimental results. Liner for Mach number 1·40.

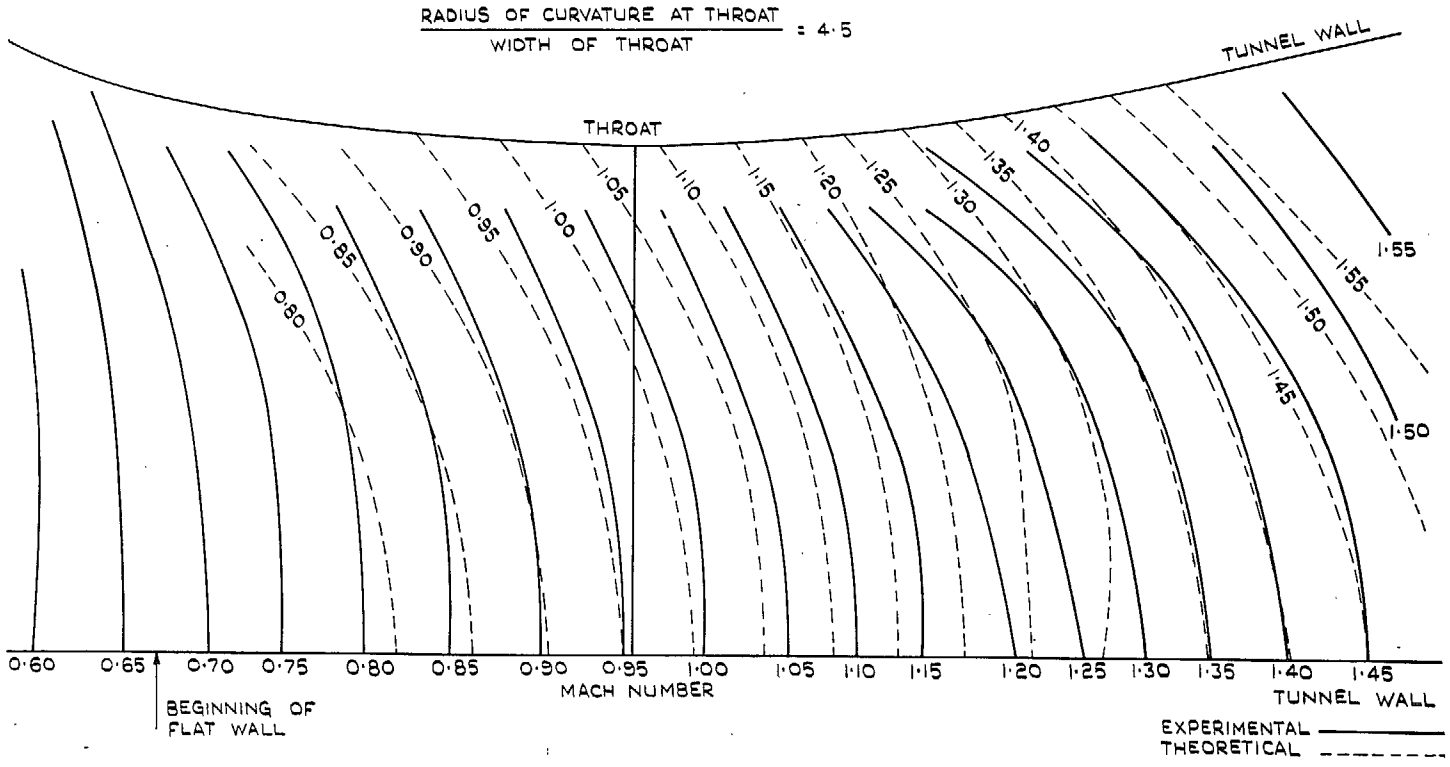

FIG. 28. Flow through a sonic throat. Comparison of theoretical and experimental results. Liner for Mach number 2·00.

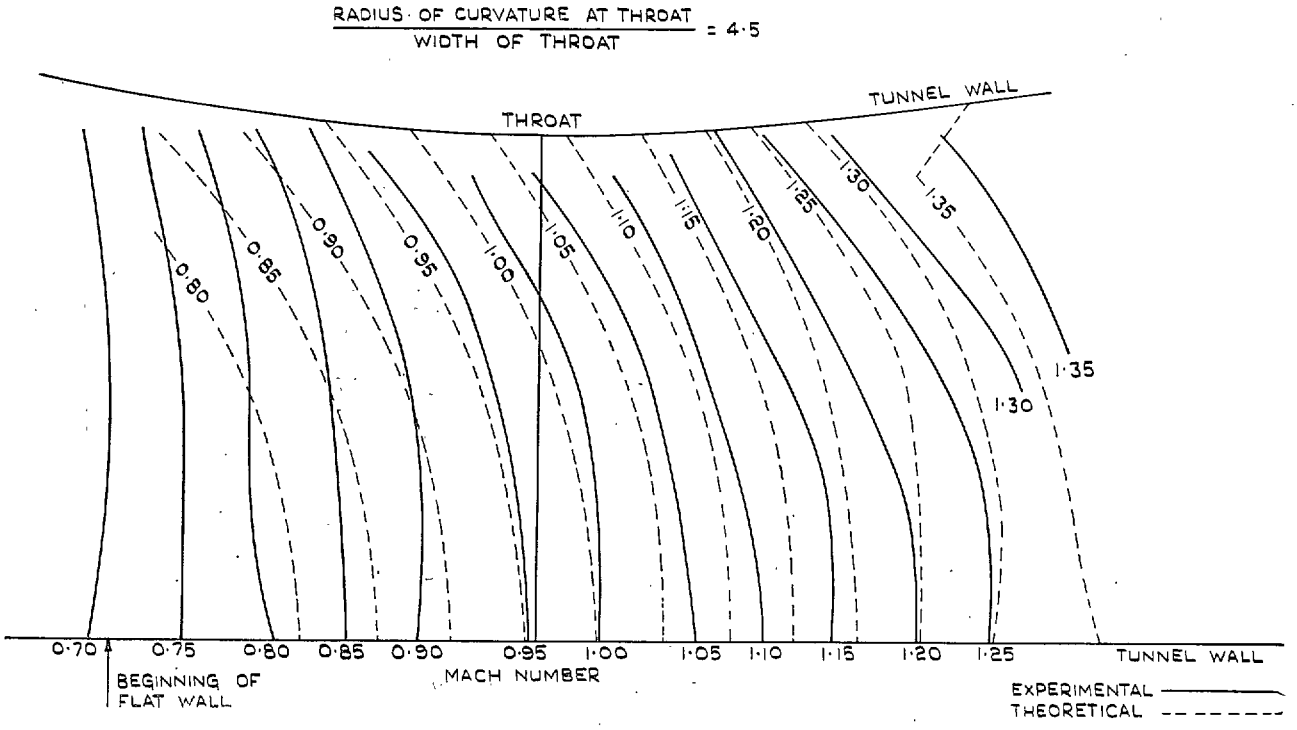

FIG. 29. Flow through a sonic throat. Comparison of theoretical and experimental results. Liner for Mach number 1·60.

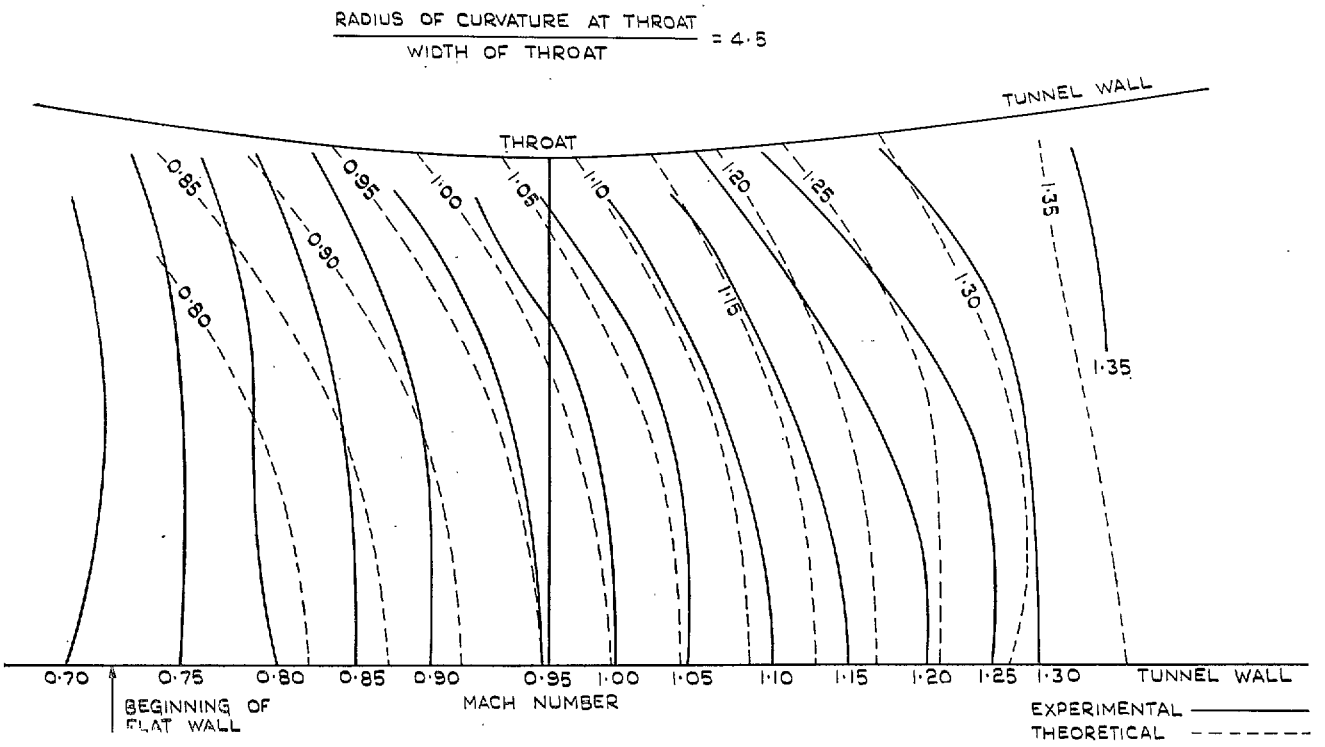

FIG. 30. Flow through a sonic throat. Comparison of theoretical and experimental results. Alternative liner for Mach number 1·60.

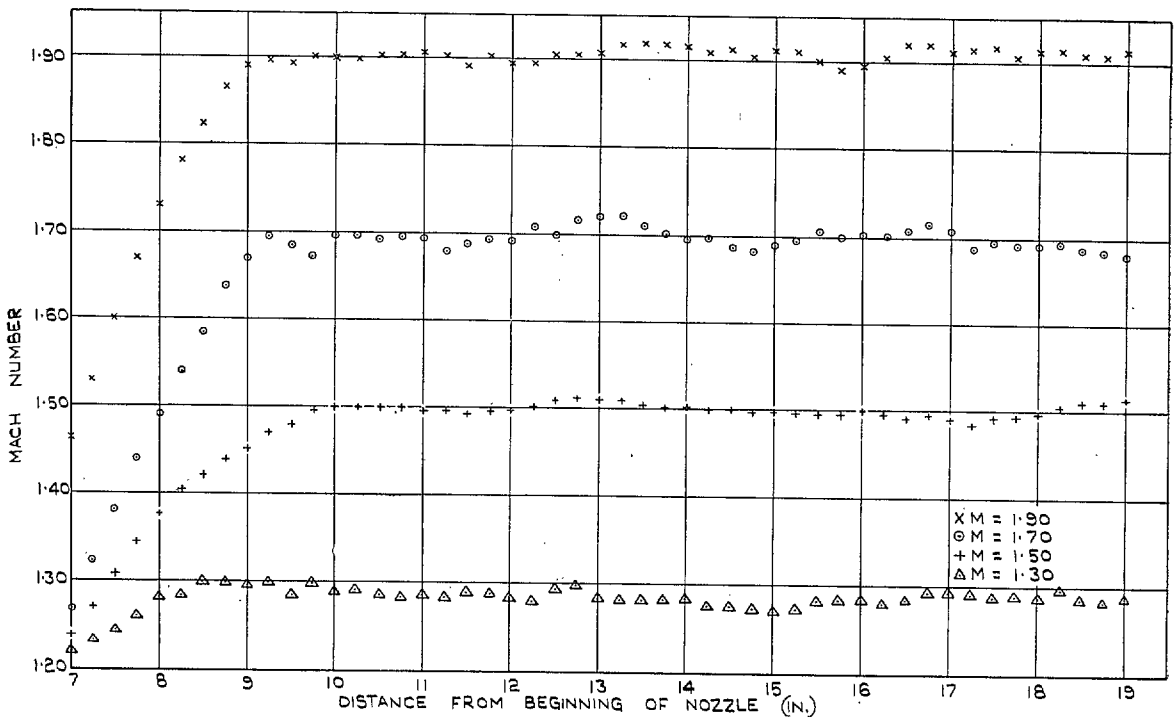

FIG. 31. Mach number distributions of derived liners : initial tests.

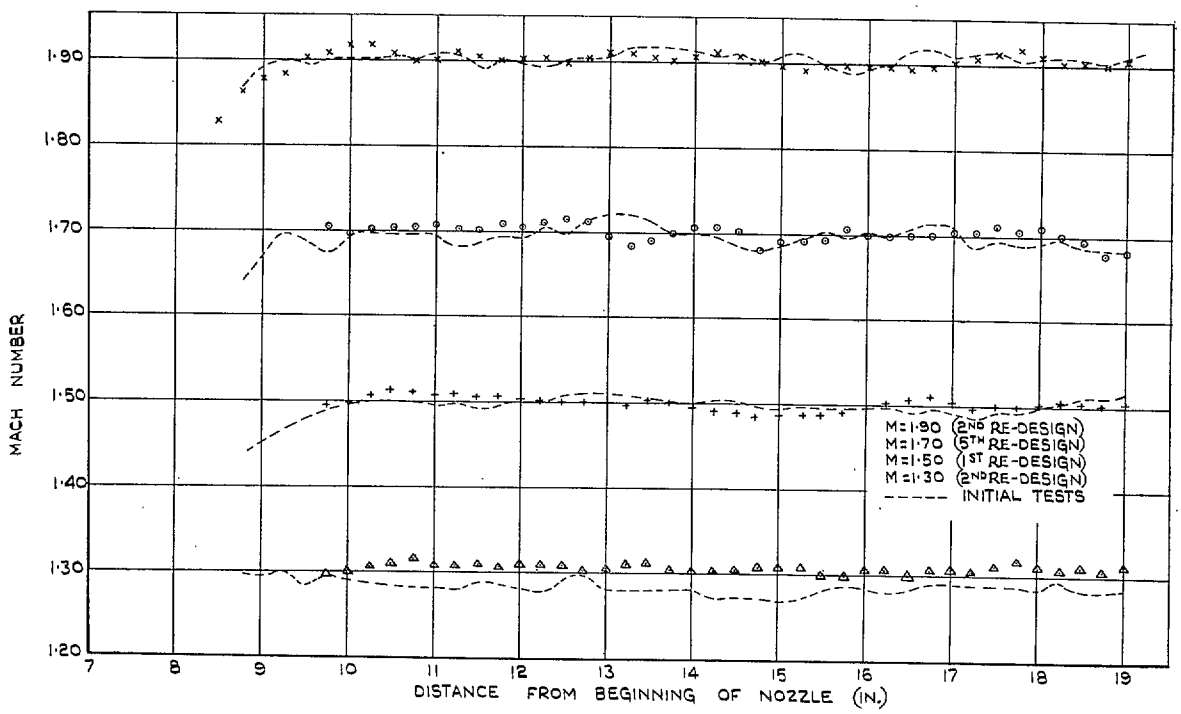

FIG. 32. Mach number distributions of derived liners : after modification.

(52567) Wt. 15/680. K9 8/53 Hw.

PRINTED IN GREAT BRITAIN

Publications of the Aeronautical Research Council

ANNUAL TECHNICAL REPORTS OF THE AERONAUTICAL RESEARCH COUNCIL (BOUND VOLUMES)

1936 Vol. I. Aerodynamics General, Performance, Airscrews, Flutter and Spinning. 40*s.* (40*s.* 9*d.*)
Vol. II. Stability and Control, Structures, Seaplanes, Engines, etc. 50*s.* (50*s.* 10*d.*)

1937 Vol. I. Aerodynamics General, Performance, Airscrews, Flutter and Spinning. 40*s.* (40*s.* 10*d.*)
Vol. II. Stability and Control, Structures, Seaplanes, Engines, etc. 60*s.* (61*s.*)

1938 Vol. I. Aerodynamics General, Performance, Airscrews. 50*s.* (51*s.*)
Vol. II. Stability and Control, Flutter, Structures, Seaplanes, Wind Tunnels, Materials. 30*s.* (30*s.* 9*d.*)

1939 Vol. I. Aerodynamics General, Performance, Airscrews, Engines. 50*s.* (50*s.* 11*d.*)
Vol. II. Stability and Control, Flutter and Vibration, Instruments, Structures, Seaplanes, etc. 63*s.* (64*s.* 2*d.*)

1940 Aero and Hydrodynamics, Aerofoils, Airscrews, Engines, Flutter, Icing, Stability and Control, Structures, and a miscellaneous section. 50*s.* (51*s.*)

1941 Aero and Hydrodynamics, Aerofoils, Airscrews, Engines, Flutter, Stability and Control, Structures. 63*s.* (64*s.* 2*d.*)

1942 Vol. I. Aero and Hydrodynamics, Aerofoils, Airscrews, Engines. 75*s.* (76*s.* 3*d.*)
Vol. II. Noise, Parachutes, Stability and Control, Structures, Vibration, Wind Tunnels 47*s.* 6*d.* (48*s.* 5*d.*)

1943 Vol. I. (*In the press.*)
Vol. II. (*In the press.*)

ANNUAL REPORTS OF THE AERONAUTICAL RESEARCH COUNCIL—

1933–34	1*s.* 6*d.* (1*s.* 8*d.*)	1937	2*s.* (2*s.* 2*d.*)
1934–35	1*s.* 6*d.* (1*s.* 8*d.*)	1938	1*s.* 6*d.* (1*s.* 8*d.*)
April 1, 1935 to Dec. 31, 1936.	4*s.* (4*s.* 4*d.*)	1939–48	3*s.* (3*s.* 2*d.*)

INDEX TO ALL REPORTS AND MEMORANDA PUBLISHED IN THE ANNUAL TECHNICAL REPORTS, AND SEPARATELY—

April, 1950 - - - - R. & M. No. 2600. 2*s.* 6*d.* (2*s.* 7½*d.*)

AUTHOR INDEX TO ALL REPORTS AND MEMORANDA OF THE AERONAUTICAL RESEARCH COUNCIL—

1909–1949. R. & M. No. 2570. 15*s.* (15*s.* 3*d.*)

INDEXES TO THE TECHNICAL REPORTS OF THE AERONAUTICAL RESEARCH COUNCIL—

December 1, 1936 — June 30, 1939.	R. & M. No. 1850.	1*s.* 3*d.* (1*s.* 4½*d.*)
July 1, 1939 — June 30, 1945.	R. & M. No. 1950.	1*s.* (1*s.* 1½*d.*)
July 1, 1945 — June 30, 1946.	R. & M. No. 2050.	1*s.* (1*s.* 1½*d.*)
July 1, 1946 — December 31, 1946.	R. & M. No. 2150.	1*s.* 3*d.* (1*s.* 4½*d.*)
January 1, 1947 — June 30, 1947.	R. & M. No. 2250.	1*s.* 3*d.* (1*s.* 4½*d.*)
July, 1951.	R. & M. No. 2350.	1*s.* 9*d.* (1*s.* 10½*d.*)

Prices in brackets include postage.

Obtainable from

HER MAJESTY'S STATIONERY OFFICE

York House, Kingsway, London, W.C.2; 423 Oxford Street, London, W.1 (Post Orders: P.O. Box 569, London, S.E.1); 13a Castle Street, Edinburgh 2; 39, King Street, Manchester, 2; 2 Edmund Street, Birmingham 3; 1 St. Andrew's Crescent, Cardiff; Tower Lane, Bristol 1; 80 Chichester Street, Belfast, or through any bookseller